ARMY RESEARCH LABORATORY

Spin-Yaw Lockin of an Elastic Finned Projectile

by Charles H. Murphy and William H. Mermagen, Sr.

ARL-TR-3217 **August 2004**

NOTICES

Disclaimers

The findings in this report are not to be construed as an official Department of the Army position unless so designated by other authorized documents.

Citation of manufacturer's or trade names does not constitute an official endorsement or approval of the use thereof.

Destroy this report when it is no longer needed. Do not return it to the originator.

Army Research Laboratory
Aberdeen Proving Ground, MD 21005-5066

ARL-TR-3217 **August 2004**

Spin-Yaw Lockin of an Elastic Finned Projectile

Charles H. Murphy and William H. Mermagen, Sr.
Weapons and Materials Research Directorate, ARL

Report Documentation Page

Form Approved
OMB No. 0704-0188

1. REPORT DATE *(DD-MM-YYYY)*	2. REPORT TYPE	3. DATES COVERED (From - To)
August 2004	Final	January–July 2003

4. TITLE AND SUBTITLE
Spin-Yaw Lockin of an Elastic Finned Projectile

5a. CONTRACT NUMBER

5b. GRANT NUMBER

5c. PROGRAM ELEMENT NUMBER

6. AUTHOR(S)
Charles H. Murphy and William H. Mermagen, Sr.

5d. PROJECT NUMBER
AH80

5e. TASK NUMBER

5f. WORK UNIT NUMBER

7. PERFORMING ORGANIZATION NAME(S) AND ADDRESS(ES)
U.S. Army Research Laboratory
ATTN: AMSRD-ARL-WM-BC
Aberdeen Proving Ground, MD 21005-5066

8. PERFORMING ORGANIZATION REPORT NUMBER
ARL-TR-3217

9. SPONSORING/MONITORING AGENCY NAME(S) AND ADDRESS(ES)

10. SPONSOR/MONITOR'S ACRONYM(S)

11. SPONSOR/MONITOR'S REPORT NUMBER(S)

12. DISTRIBUTION/AVAILABILITY STATEMENT
Approved for public release; distribution is unlimited.

13. SUPPLEMENTARY NOTES

14. ABSTRACT
Supersonic finned projectiles carrying very long dense metallic rods have been observed to have significantly large flexing motion. The appropriate Lagrangian for a pitching, yawing, rolling, and flexing missile is derived and the powerful finite element method used to construct differential equations for finite element parameters. These differential equations for constant spin are used to calculate frequencies and damping rates of transient motion and trim response motion to missile-fixed inertia and aerodynamic forcing terms associated with inelastic deformations. The results agree with earlier results based on a much more difficult iterative integration of a complex differential equation with unusual boundary conditions. Only three elements were necessary for reasonable accuracy, although codes for five and seven elements have been prepared and exercised. The finite element ordinary differential equations allowed calculation of the time history of missile motion with varying spin and demonstrated the occurrence of spin-yaw resonance at the aerodynamic frequency and at the lowest elastic frequency.

15. SUBJECT TERMS
aeroelastic, spin-yaw lockin, finned projectile

16. SECURITY CLASSIFICATION OF:			17. LIMITATION OF ABSTRACT	18. NUMBER OF PAGES	19a. NAME OF RESPONSIBLE PERSON
a. REPORT	b. ABSTRACT	c. THIS PAGE			Gene Cooper
UNCLASSIFIED	UNCLASSIFIED	UNCLASSIFIED	UL	64	19b. TELEPHONE NUMBER (*Include area code*) 410-278-3684

Standard Form 298 (Rev. 8/98)
Prescribed by ANSI Std. Z39.18

Contents

List of Figures

List of Tables

INTENTIONALLY LEFT BLANK.

1. Introduction

Very long finned projectiles carrying very dense metallic rods have been observed to be subjected to large inelastic deformations during hypersonic flight (*1*). Spark shadowgraphs of these projectiles have shown elastic bending motion with amplitudes as large as the rod's radius (*2*). It has been conjectured that the cause of the inelastic deformation was the bending loads associated with pitching and yawing motion at resonant spin frequencies. These frequencies would be near to the aerodynamic frequency of a rigid projectile or the elastic frequencies of the rod.

Spinning motion at a resonant frequency can be caused by a nonlinear roll moment associated with the roll orientation of the fins or by mass asymmetry due to damage or poor construction of the projectile. This spin-yaw lockin mechanism has been discussed for a rigid missile by several authors (*3*–*7*).

The linear flight motion of an elastic missile has been considered in references (*8*–*13*). In reference (*11*), a very simple theoretical model of a projectile composed of three components connected by two bent mass-less elastic beams was used to approximate an elastic missile. For appropriate selection of beam parameters spin-yaw lockin was demonstrated and large amplitude oscillations occurred. In references (*12*) and (*13*), the correct linear partial-differential equation for a continuously elastic missile was derived, and special solutions for harmonic transient motion and trim motion were obtained. A nonlinear roll moment was shown to be capable of producing equilibrium spin near resonance. Although the lateral motion of the pitching and yawing missile was linearized, it was necessary to retain the quadratic terms in the roll equation. A time history of motion going to lockin was not obtained at that time. It is the purpose of this report to compute such a time history by use of the finite element method (FEM) (*14*).

The lateral motion of a symmetric rigid missile has often been described by complex variables (*15*), and complex variables were used in references (*8*) and (*11*–*13*) to describe the lateral flexing motion of the rotationally symmetric rod. The equations of motion of a spinning missile are usually derived by vector analysis and Newtonian mechanics, but FEM equations for elastic bodies require the use of the more sophisticated Lagrangian mechanics. The Lagrangian of a system must be stated in body-fixed coordinates. Separate differential equations in the two lateral directions can be obtained from the appropriate Lagrangian. Pairs of equations are combined and complex variables introduced to yield half as many complex equations.

If five elements are used to describe the pitching and flexing motion of the missile, 20 parameters, usually called connectors, are introduced and 25 second-order differential equations and one first order differential equation are required. The introduction of complex angles and complex connections reduce this system to 12 second-order complex differential equations and two real differential equations.

2. Coordinate System

The elastic missile is assumed to consist of a very heavy elastic circular rod of fineness ratio, L, and mass, m, embedded in a very light symmetric aerodynamic structure that may be longer than the rod. The rod's axial moment of inertia is I_x and its transverse moment of inertia about its center is I_{t0}. The rod's diameter can vary over its length, and its maximum diameter will be denoted by "d." All distances will be expressed as multiples of the rod diameter and its length is Ld. A nose windshield of length $x_{23}d$ may be attached to the forward end of the rod, and the fins may extend beyond the end of the rod at a distance of $x_{01}d$. Thus, the rod is located between $x_1 = -L/2$ and $x_2 = L/2$, while the aerodynamic structure extends from $x_0 = x_1 - x_{01}$ to $x_3 = x_2 + x_{23}$.

An earth-fixed coordinate system will be used with the X_e-axis oriented along the initial direction of the missile's velocity vector. The Z_e-axis is downward-pointing and the Y_e-axis is determined by the right hand rule. A nonrotating coordinate system, XYZ is then defined with origin always at the center of the rod and the X-axis tangent there. The X-axis pitches through the angle, θ, and yaws through the angle, ψ, with respect to the X_e-axis. Body-fixed coordinates XY_b-Z_b are now defined for which the Y_b-Z_b axes rotate with the missile through the roll angle, ϕ, with respect to the Y-Z axes.

We will conceptually slice the missile into a large number of thin disks perpendicular to the X-axis with thickness, dx. When the rod flexes, the disks shift laterally perpendicular to the X-axis and cant to be perpendicular to the centerline of the disks. This canting action neglects the shear deformation of the rod, and this constraint is called the Bernoulli assumption (*14*). The lateral displacement of a disk has body-fixed coordinates δ_{by} and δ_{bz}, and the disk is canted at angles Γ_{by} and Γ_{bz}.

$$\Gamma_{by} = \frac{\partial \delta_{by}}{\partial x}; \qquad \Gamma_{bz} = \frac{\partial \delta_{bz}}{\partial x}. \tag{1}$$

It important to note that at the central disk

$$\delta_{by}(0,t) = \delta_{bz}(0,t) = \Gamma_{by}(0,t) = \Gamma_{bz}(0,t) = 0. \tag{2}$$

Reference (*12*) used the nonspinning elastic coordinate system with XYZ axes $(\phi = 0)$. The lateral displacements of a disk in this elastic coordinate system are shown in figures 1 and 2 and can be computed from body-fixed quantities.

$$\delta_E = \delta_{Ey} + i\delta_{Ez} = \left(\delta_{by} + i\delta_{bz}\right) e^{i\phi}, \tag{3}$$

and

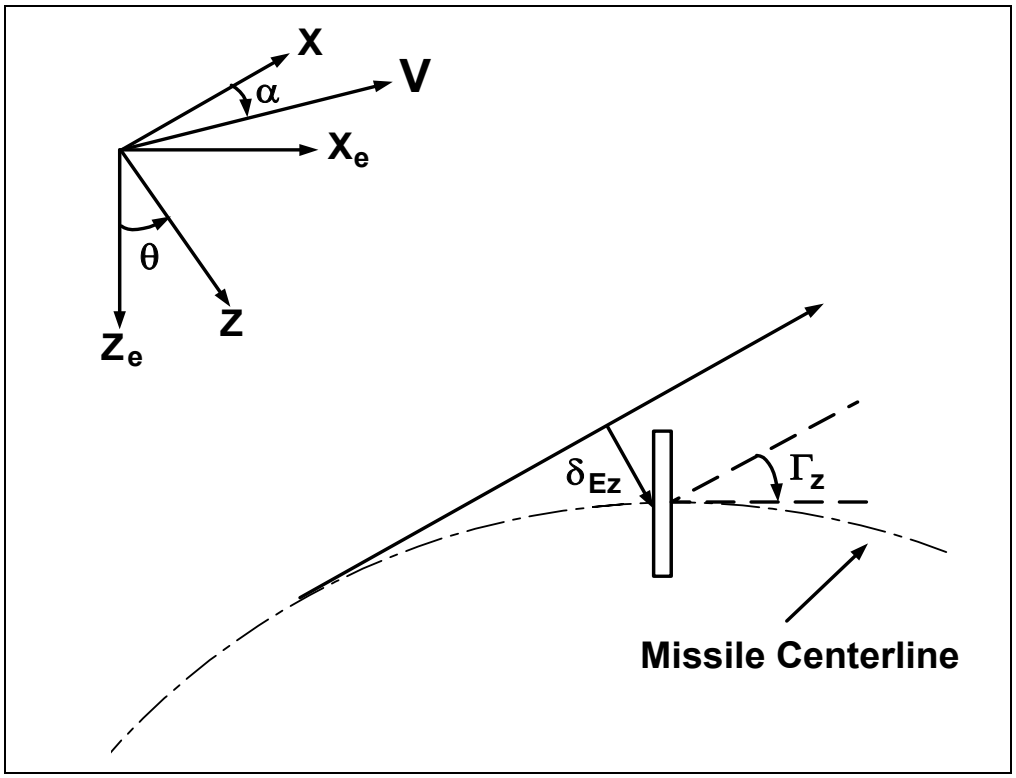

Figure 1. X-Z coordinates of cross-sectional disk.

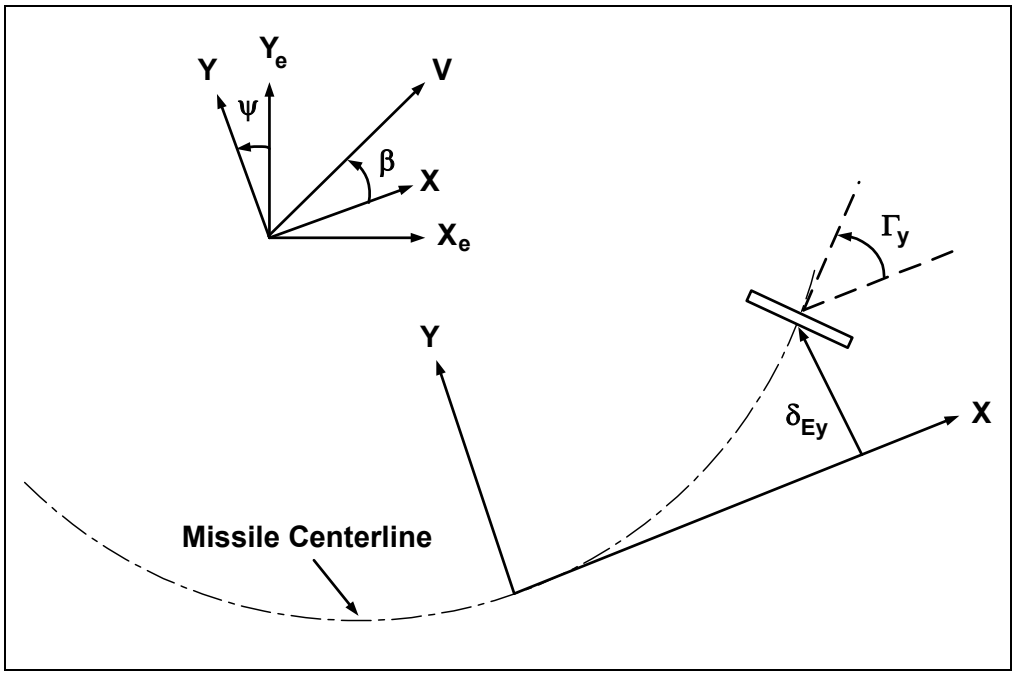

Figure 2. X-Y coordinates of cross-sectional disk.

$$\Gamma = \Gamma_y + i\Gamma_z = \left(\Gamma_{by} + i\Gamma_{bz}\right)\, e^{i\phi}. \tag{4}$$

The earth-fixed coordinates of the central disk are $x_e, y_e,$ and z_e, and the earth-fixed coordinates of the other disks are computed in terms of the central disk earth-fixed coordinates, their body-fixed displacements, and the Euler angles $\theta,\ \psi,$ and ϕ.

$$x_{de} = x_e + x\left[1 - \left(\psi^2 + \theta^2\right)/2\right] - \psi\, \mathrm{Re}\left\{\left(\delta_{by} + i\delta_{bz}\right)e^{i\phi}\right\} + \theta\, \mathrm{Im}\left\{\left(\delta_{by} + i\delta_{bz}\right)e^{i\phi}\right\}, \tag{5}$$

$$y_{de} = y_e + x\psi + \mathrm{Re}\left\{\left(\delta_{by} + i\delta_{bz}\right)e^{i\phi}\right\}, \tag{6}$$

and

$$z_{de} = z_e - x\theta + \mathrm{Im}\left\{\left(\delta_{by} + i\delta_{bz}\right)e^{i\phi}\right\}. \tag{7}$$

$y_e,\ z_e,\ \theta,\ \psi,\ \delta_{by},\ \delta_{bz}$ and their derivatives are assumed to be small quantities, but x_e and $\dot{x}_e$ are not small. Lagrangian dynamics yields the correct linearized differential equations for these six variables when the kinetic energy expansion retains all quadratic terms in these variables. Thus, equations 6 and 7 consist of only linear terms, but equation 5, which contains x_e, retains quadratic terms in these variables. The coefficient of x in equation 5, for example, is the quadratic form of the cosine of the angle between the X_e-axis and the X-axis.

The angular velocity of the central disk in the body-fixed coordinates is

$$p = \dot{\phi} - \dot{\psi}\theta, \tag{8}$$

$$q_b = \mathrm{Re}\left\{\left(\dot{\theta} + i\dot{\psi}\right)\, e^{-i\phi}\right\}, \tag{9}$$

and

$$r_b = \mathrm{Im}\left\{\left(\dot{\theta} + i\dot{\psi}\right)\, e^{-i\phi}\right\}. \tag{10}$$

The angular velocity of any other disk along axes aligned with the disk's axes of symmetry is

$$p_d = p\left(1 - \Gamma\bar{\Gamma}/2\right) + q_d\Gamma_{by} + r_d\Gamma_{bz} = p + \mathrm{Re}\left\{\left(\dot{\theta} + i\dot{\psi} - \dot{\phi}\Gamma/2 + i\dot{\Gamma}\right)\, \bar{\Gamma}\right\}, \tag{11}$$

$$q_d = q_b - \dot{\Gamma}_{bz} - \dot{\phi}\Gamma_{by} = \mathrm{Re}\left\{\left(\dot{\theta} + i\dot{\psi} + i\dot{\Gamma}\right)\, e^{-i\phi}\right\}, \tag{12}$$

and

$$r_d = r_b + \dot{\Gamma}_{by} - \dot{\phi}\Gamma_{bz} = \mathrm{Im}\left\{\left(\dot{\theta} + i\dot{\psi} + i\dot{\Gamma}\right)\, e^{-i\phi}\right\}. \tag{13}$$

3. Motion of Central Disk

The mass of each circular disk is $(m/L)\ \rho_1(x)\ dx$; its roll moment of inertia is $2a_d(md^2)\ \rho_2(x)\ dx$, and its transverse moment of inertia is $a_d(md^2)\ \rho_2(x)\ dx$, where a_d is $(16L)^{-1}$. $\rho_1(x)$ and $\rho_2(x)$ describe the variation of mass and moments of inertia along the rod, and both become unity for a homogeneous rod with constant diameter. The kinetic energy of a disk is therefore

$$T_d dx = \left[\left(md^2\rho_1/2L\right)\left(\dot{x}_{de}^2 + \dot{y}_{de}^2 + \dot{z}_{de}^2\right) + \left(a_d md^2\rho_2/2\right)\left(2p_d^2 + q_d^2 + r_d^2\right)\right] dx\,. \tag{14}$$

The total kinetic energy of the missile can be obtained by integrating T_d over the length of the rod:

$$T = \int_{x_1}^{x_2} T_d dx = T_R + md^2\left(T_{11} + T_{12}\right) + \left(md^2/2L\right)\left(T_{21} + T_{22}\right), \tag{15}$$

where
$$T_R = \left(md^2/2\right)\left(\dot{x}_e^2 + \dot{y}_e^2 + \dot{z}_e^2\right) + I_x p^2/2 + I_{t0}\left(\dot{\psi}^2 + \dot{\theta}^2\right)/2 + md^2 x_c\left[\dot{y}_e\dot{\psi} - \dot{z}_e\dot{\theta} - \dot{x}_e\left(\psi\dot{\psi} + \theta\dot{\theta}\right)\right],$$

$$T_{11} = -\dot{x}_e\,\mathrm{Re}\left\{\left(\psi + i\theta\right)\dot{\delta}_c + \left(\dot{\psi} + i\dot{\theta}\right)\delta_c\right\},$$

$$T_{12} = \mathrm{Re}\left\{\left(\dot{y}_e - i\dot{z}_e\right)\dot{\delta}_c + \left(\dot{\psi} + i\dot{\theta}\right)\left(\dot{J}_6 + J_8\right)\right\},$$

$$T_{21} = \int_{x_1}^{x_2}\left(\dot{\delta}_{Ey}^2 + \dot{\delta}_{Ez}^2\right)\rho_1 dx + \left(a_d L\right)\int_{x_1}^{x_2}\left(\dot{\Gamma}_y^2 + \dot{\Gamma}_z^2\right)\rho_2 dx,$$

$$T_{22} = 2\dot{\phi}\left(a_d L\right)\mathrm{Re}\left\{\int_{x_1}^{x_2}\left(2i\dot{\Gamma} - \dot{\phi}\Gamma\right)\overline{\Gamma}\rho_2 dx\right\},$$

and

$$x_c = \left(1/L\right)\int_{x_1}^{x_2} x\rho_1 dx\,.$$

The y_e and z_e components of the central disk velocity can be approximated by linear relations in angles of pitch and yaw with respect to inertia axes (θ, ψ) and angles of attack and sideslip with respect to the velocity vector (α, β) as shown in figures 1 and 2. The magnitude of the velocity vector is V.

$$\dot{y}_e = \left(V/d\right)\ \left(\beta + \psi\right), \tag{16}$$

and

$$\dot{z}_e = (V/d)\ (\alpha - \theta). \tag{17}$$

Equations 16 and 17 can be written as a single complex equation:

$$\dot{y}_e + i\dot{z}_e = (V/d)\ (q_l + q_{le}), \tag{18}$$

where $q_l = \beta + i\alpha$ and $q_{le} = \psi - i\theta$.

In reference (*12*), the linear aerodynamic force loading is expressed in terms of three force distribution functions, $c_D(x)$, $c_{f1}(x)$, and $c_{f2}(x)$ and the base pressure coefficient, C_{Dbp}, plus a body-fixed force associated with possible bent fins. Because the lateral motion of the missile is quite small, $\dot{q}_l \cong -\dot{q}_{le}$ and the aerodynamic damping force terms in the aerodynamic loading on the aerodynamic structure can be combined. This aerodynamic loading in nonrotating elastic coordinates is

$$\frac{dF_x}{dx} = -g_l c_D(x), \tag{19}$$

$$\frac{dF_y}{dx} + i\frac{dF_z}{dx} = -g_l \left[\begin{array}{l} c_{f1}(x)\ \left[q_l - \Gamma - \Gamma_{BF}(x)\ e^{i\phi} + \left(\dot{\delta}_E - x\dot{q}_l \right)\ (d/V) \right] \\ \qquad + c_{f2}(x)\ \left(2\dot{q}_l - \dot{\Gamma} - i\dot{\phi}\Gamma_{BF}(x)\ e^{i\phi} \right)\ (d/V) \end{array} \right], \tag{20}$$

and

$$F_{xbp} = -g_l C_{Dpb}. \tag{21}$$

The total aerodynamic force acting on the aerodynamic structure is given by the integrals of equations 19 and 20 and by adding the base drag of equation 21 to the axial force,

$$F_x = -g_l C_D = -g_l \left[\int_{x_0}^{x_3} c_D(x)\,dx + C_{Dbp} \right], \tag{22}$$

and

$$F = -g_l \left[c_l q_l + c_2 (\dot{q}_l d/V) - C_{NBF} e^{i\phi} - J_1(t) - \dot{J}_2(t)\ (d/V) \right], \tag{23}$$

where various functions are defined in appendices A and B.

The primary components of drag are head drag and base pressure drag. The third component is skin friction drag that is ~15% of the total drag and will be neglected in this report to simplify the FEM calculations.

Similarly, the total aerodynamic moment about the rod's center can be computed from the transverse aerodynamic force and a small axial force contribution:

$$M = M_y + iM_z$$
$$= -i(g_1 d)\left[c_3 q_1 + c_4(\dot{q}_1 d/V) - C_{MBF} e^{i\phi} - J_3(t) - \dot{J}_4(t)(d/V) - J_5(t)\right]. \quad (24)$$

The motion of the central disk is described by the variables x_e, y_e, z_e, ϕ, ψ, and θ. The motion of any other section on the aerodynamic structure located at x with thickness dx is the sum of this motion plus its motion relative to the central disk. The work done on any section caused by motion of the central disk is

$$(dW_{cd})_x\, dx = dQ_{1x}dx_e + dQ_{1y}dy_e + dQ_{1z}dz_e + dQ_{2x}d\phi + dQ_{2y}dq_{1ey} + dQ_{2z}dq_{1ez}, \quad (25)$$

where the sectional generalized forces are defined in appendix B.

The total generalized forces can be obtained by integrating the sectional generalized forces and adding the work done by the base pressure drag. These are also given in appendix C.

The linearized Lagrangian differential equation for x_e and ϕ gives the usual drag and spin equation,

$$m\dot{V} \cong m\ddot{x}_e = -g_1 C_D, \quad (26)$$

and

$$I_x\ddot{\phi} = M_x. \quad (27)$$

The Lagrangian differential equation for z_e can be multiplied by i and added to the Lagrangian differential equation for y_e to yield a single second-order differential equation in complex variables. Next, the Lagrangian differential equation for θ can be multiplied by i and subtracted from the Lagrangian differential equation for ψ,

$$m\left[V(\dot{q}_1 + q_2) + \dot{V}q_1 + \ddot{\delta}_c d + \dot{q}_2 x_c d\right] = F \quad (28)$$

and

$$\left(I_{t0} + md^2x_c^2\right)\dot{q}_2 - i\dot{\phi}I_x q_2 + md^2\left[\ddot{J}_6 + \dot{J}_8 + x_c\ddot{\delta}_c\right] = -iM - x_c F d, \quad (29)$$

where $x_c = (1/L)\int_{x_1}^{x_2} x\rho_1 dx$, $\delta_c = (1/L)\int_{x_1}^{x_2} \delta_E \rho_1 dx$, and $q_2 = \dot{q}_{1e}$.

These differential equations for $x_c = 0$ are the same as those derived by Newtonian mechanics in reference (*12*). Equations 28 and 29 contain eight integrals of δ_E and Γ. Three of these are integrals of dynamics properties (δ_c, J_6, J_8) over the rod (x_1, x_2) and five are integrals over aerodynamic properties $(J_1, J_2, J_3, J_4, J_5)$ over the aerodynamic structure (x_0, x_3).

For constant spin and velocity, a rigid unbent missile with its center of mass at the rod center, equations 28 and 29 predict a simple epicyclic angular motion:

$$q_1 = K_{10} e^{\lambda_1 t + i\phi_1} + K_{20} e^{\lambda_2 t + i\phi_2} , \tag{30}$$

where $\dot{\phi}_m = \dot{\phi} I_x / 2I_t \pm \sqrt{-(g_1 d / I_t)\, c_3 + (\dot{\phi} I_x / 2I_t)^2}$.

For zero spin, $\dot{\phi}_1 = -\dot{\phi}_2 = \omega_R$, where $\omega_R = \sqrt{(g_1 d / I_t)|c_3|}$.

---

4. FEM

The rod is assumed to be represented by the sum of an inelastic bent component rotating with the missile and an elastic deformation,

$$\delta_E(x,t) = \delta_{EB}(x)\ e^{i\phi} + \tilde{\delta}_E(x,t)\ ; \qquad x_1 \le x \le x_2 , \tag{31}$$

and

$$\delta_b(x,t) = \delta_{EB}(x) + \tilde{\delta}_b(x,t)\ ; \qquad x_1 \le x \le x_2 , \tag{32}$$

where $\delta_{EB}(0) = \dfrac{d\delta_{EB}(0)}{dx} = 0$.

Because the aerodynamic structure is rigidly attached to the rod,

$$\delta_E(x,t) = \delta_E(x_1,t) + (x - x_1)\ \Gamma(x_1,t)\ ; \qquad x_0 \le x \le x_1 , \tag{33}$$

and

$$\delta_E(x,t) = \delta_E(x_2,t) + (x - x_2)\ \Gamma(x_2,t)\ ; \qquad x_2 \le x \le x_3 . \tag{34}$$

The motion of the elastic component of the rod is controlled by the elasticity of the rod and the aerodynamic force acting on it.

FEM is a very powerful method for calculating the time history of the elastic flexing motion. The rod is divided into n_j elements of length $L_e = L / n_j$. The shape of the j-th element is given by a linear combination of third-order Hermitian polynomials (see appendix C).

$$\tilde{\delta}_{by}(x,t) = \sum_1^4 \hat{q}_{bpy}(t)\ N_p(z) , \tag{35}$$

and

$$\tilde{\delta}_{bz}(x,t) = \sum_{1}^{4} \hat{q}_{bpz}(t)\, N_p(z), \tag{36}$$

where $x = L_e(z + z_j)$; $z_j = x_1/L_e + j - 1$ $0 \le z \le 1$.

The coefficients of the polynomials are functions of time and are called connectors. The first two are the deflection and slope of the left end of the element and the third and fourth are the deflection and slope of the right end. To ensure continuity in deflection and slope at junction points, the corresponding pairs of connectors are equal. We will consider only an odd number of elements and require that the connecters of the central element satisfy equation 2.

$$\hat{q}_{b3} = 5\hat{q}_{b1} + L_e\hat{q}_{b2}, \tag{37}$$

and

$$\hat{q}_{b4} = 24L_e^{-1}\hat{q}_{b1} + 5\hat{q}_{b2}, \tag{38}$$

where $\hat{q}_{bq} = \hat{q}_{bqy} + i\hat{q}_{bqz}$.

For n_j elements, there are $2n_j$ independent complex connectors. It is convenient to let the index for the connectors run from 3 to n_t, where $n_t = 2n_j + 2$. The usual FEM procedure calculates the elastic parts of the integrals in equations 28 and 29 by first obtaining integrals over each element. These are linear functions of that element's four connector functions. Due to equations 37 and 38, the central element has only two independent connector functions, and the next adjacent element connector functions are related to them. Integrals for these elements are specially computed. The desired elastic integrals are sums of these subintegrals and are linear combinations of the $2n_j$ complex connector functions. The three integrals can be written as

$$\delta_c = L^{-1}\sum_{3}^{n_t} a_{1n}q_n + \delta_{cB}e^{i\phi}, \tag{39}$$

$$J_6 = L^{-1}\sum_{3}^{n_t} a_{2n}q_n + J_{6B}e^{i\phi}, \tag{40}$$

and

$$J_8 = a_d\sum_{3}^{n_t} b_{2n}\left(\dot{q}_n - 2i\dot{\phi}q_n\right) - i\dot{\phi}J_{8Bl}e^{i\phi}, \tag{41}$$

where $q_n = q_{bn}e^{i\phi}$.

The five integrals have contributions from the aerodynamic structure extensions as well as from each element,

$$J_1 + \dot{J}_2\,(d/V) = \sum_3^{n_t}\left[\left(f_{1n} + f_{a1n}\right) q_n + \left(g_{1n} + g_{a1n}\right)\left(\dot{q}_n d/V\right)\right] + \left[J_{1B} + i\left(\dot{\phi} d/V\right) J_{2B}\right] e^{i\phi}, \tag{42}$$

$$J_3 + \dot{J}_4\,(d/V) = \sum_3^{n_t}\left[\left(f_{2n} + f_{a2n}\right) q_n + \left(g_{2n} + g_{a2n}\right)\left(\dot{q}_n d/V\right)\right] + \left[J_{3B} + i\left(\dot{\phi} d/V\right) J_{4B}\right] e^{i\phi}, \tag{43}$$

and

$$J_5 = \sum_3^{n_t}\left(-C_D a_{1n} L^{-1} + h_{an}\right)\, q_n + J_{5B} e^{i\phi}. \tag{44}$$

Expressions for δ_{cB}, J_{kB}, h_{an} and all FEM coefficients in equations 39–44 for 1, 3, 5, and 7 elements are given in appendices A, D, and E.

Equations 39–44 can be used with equations 28 and 29 to write these two complex differential equations in a standard format:

$$\sum_{n=1}^{n_t}\left[R_{mn}\ddot{q}_n + \left(S_{mn} + i\dot{\phi} S^*_{mn}\right)\,\dot{q}_n + \left(T_{mn} + i\dot{\phi} T^*_{mn}\right)\, q_n\right] = t_m \exp\,\left(i\phi\right). \tag{45}$$

The coefficients for m = 1, 2 are given in appendix F.

5. Flexing Motion

In order to derive the equations for flexing motion, the kinetic energy given by equation 15 must be expressed in terms of the rigid-body parameters, plus the connector functions. The usual FEM process is used to express T_{2j} in terms of two matrices, two vectors, and two constants.

$$T_{21} = \sum_3^{n_t}\sum_3^{n_t} k_{mn}\left[\,\dot{q}_{my}\dot{q}_{ny} + \dot{q}_{mz}\dot{q}_{zn}\right] - 2\,\mathrm{Re}\left\{i\dot{\phi} e^{-i\phi}\sum_3^{n_t} k_{Bm}\dot{q}_m\right\} + \dot{\phi}^2 I_{xB1} L\,, \tag{46}$$

and

$$T_{22} = 2\dot{\phi} a_d L\,\mathrm{Re}\left\{\sum_3^{n_t}\sum_3^{n_t} b_{mn}\left(2i\dot{q}_m - \dot{\phi} q_m\right)\bar{q}_n + 2ie^{-i\phi}\sum_3^{n_t}\bar{b}_{Bm}\left(\dot{q}_m + 2i\dot{\phi} q_m\right)\right\} + \dot{\phi}^2 I_{xB2} L\,, \tag{47}$$

where I_{xB1}, I_{xB2} are defined in appendix A and $k_{mn}, k_{Bn}, b_{mn}, b_{Bn}$ are defined in Appendix G.

The potential energy stored by an elastic deformation is

$$\text{P.E.} = (1/2)\int_{x_1}^{x_2} (EI/d)\left[\left(\frac{\partial^2 \tilde{\delta}_{by}}{\partial x^2}\right)^2 + \left(\frac{\partial^2 \tilde{\delta}_{bz}}{\partial x^2}\right)^2\right] dx\,, \tag{48}$$

where $E(x)\ I(x) = E_0 I_0 \rho_3(x)$.

E_0 and I_0 are values of Young's modulus and the area moment of inertia at the rod's center. $\rho_3(x)$ gives the variation of their product along the rod. For a homogeneous rod with constant diameter, the product is $E_0 I_0$. The potential energy integral can be replaced by a sum of integrals over each of the n_j elements. After integrating over each element, the results can be summed to yield a linear combination of the $4n_j$ real connectors,

$$V = \left(\ md^2\omega_0^2/2L\right) \sum_{m=3}^{n_t}\sum_{n=3}^{n_t}\left(q_{bmy}q_{bny} + q_{bmz}q_{bnz}\right) c_{mn}\,, \tag{49}$$

where $\omega_0^2 = E_0 I_0 / md^3$, c_{mn} are defined in appendix G.

The work done on the rod by this elastic force can be expressed in terms of generalized force terms,

$$dW_E = \left(\ md^2/L\right) \omega_0^2 \sum_{m=3}^{n_t}\left[\ Q_{Emy}dq_{bmy} + Q_{Emz}dq_{bmz}\right], \tag{50}$$

where $Q_{Emy} + iQ_{Emz} = -\sum_{n=3}^{n_t} c_{mn} q_{bn}$.

The Kelvin-Voight elastic damping force (*16*), which is proportional to the time derivative of the elastic shear force, has generalized force terms:

$$dW_D = \left(\ md^2/L\right) \omega_0^2 \sum_{m=3}^{n_t}\left[\ Q_{Dmy}dq_{bmy} + Q_{Dmz}dq_{bmz}\right], \tag{51}$$

where $Q_{Dmy} + iQ_{Dmz} = -\left[\ 2\hat{k}/\omega_1\right) \sum_{n=3}^{n_t} c_{mn}\dot{q}_{bn}$, $\omega_1 = (4.730/L)^2\,\omega_0$.

The scale factor $2\omega_1^{-1}$ is selected so that $\hat{k} = 1$ corresponds to critical damping of the first elastic mode.

The external aerodynamic force is divided between the force acting on the rod and the force acting on the aerodynamic structure extensions at the ends of the rod. The total work done on the missile is the sum of the work done by these forces.

$$
\begin{aligned}
dW_A &= \sum_{j=1}^{n_j} \left[\, dW_{Aj} + dW_{an_j} \, \right] \\
&= (g_1 d) \sum_{m=3}^{n_t} \left[\, Q_{Amy} dq_{bmy} + Q_{Amz} dq_{bmz} \, \right],
\end{aligned}
\tag{52}
$$

where $Q_{Amy} + iQ_{Amz} = \sum_{n=3}^{n_t} \left[\left(f_{mn} + f_{amn} \right) q_n + \left(g_{mn} + g_{amn} \right) \dot{q}_n \right] e^{-i\phi} + f_{Bm} + f_{aBm} + i\dot{\phi} \left(g_{Bm} + g_{aBm} \right)$

and $f_{mn}, g_{mn}, f_{amn}, g_{amn}, f_{Bm}, g_{Bm}, f_{aBm}, g_{aBm}$ are defined in appendix G.

Equations 50–52, in conjunction with the kinetic energy defined by equations 15, 46, and 47, can be used to derive the $4n_j$ Lagrangian differential equations for the q_{bmy}, q_{bmz}'s for $m = 3,\ 4, \ldots 2n_j + 2$. The equation for q_{bmz} should be multiplied by i and added to the corresponding equation for q_{bmy} to yield $2n_j$ complex differential equations for the complex variables $q_{bm.}$. If the q_{bm} are replaced by q_m in each equation, the result has the standard form given by equation 45, where the $14n_j$ complex coefficients for $m = 3,\ 4 \ldots 2n_j + 2$ are given in appendix F.

6. Special Solutions

A rigid symmetric finned missile flying with constant spin has two natural frequencies: $\dot{\phi}_{1R}$ and $\dot{\phi}_{2R}$, where $\dot{\phi}_{1R} \cong -\dot{\phi}_{2R}$. For zero spin, each of the flexure frequencies would give rise to two coning frequencies, $\pm\omega_K$. The frequencies present in the motion of an elastic projectile would form an infinite sequence, where the first two would be related to $\dot{\phi}_{1R}$ and $\dot{\phi}_{2R}$, while the later ones would evolve from $\pm\omega_K$, i.e., $\dot{\phi}_{2K+1} \cong \omega_K$; $\dot{\phi}_{2K+2} \cong -\omega_K$. The odd numbered modes have positive frequencies and are called positive modes, while the even numbered modes are called negative modes. For nonzero spin, the pairs of frequencies would no longer be equal in magnitude.

Transient harmonic solutions of the homogeneous constant spin version of equation 45 have the form

$$
q_m = q_{mk} e^{iAt} \qquad A = A_k \qquad k = 1,\ 2,\ 3, \ldots 2\left(2n_j + 1\right). \tag{53}
$$

After substituting equation 53 into equation 45, a set of linear homogeneous algebraic equations is derived, which is specified by an $n_t \times n_t$ matrix,

$$u_{mn} = A^2 R_{mn} + A\left(S_{mn} + i\dot{\phi} S^*_{mn} \right) + T_{mn} + i\dot{\phi} T^*_{mn} . \tag{54}$$

For n_j elements, there are $2n_j + 1$ pairs of positive and negative frequencies. The lowest frequency pair is related to the two aerodynamic frequencies and the other $2n_j$ pairs are approximations of first $2n_j$ elastic frequencies of the infinite set of frequencies for the elastic rod.

The paired frequencies are equal in magnitude when spin is zero but the positive frequency has a larger magnitude when spin is positive. For an elastic beam considered by Geradin and Rixen (*14*), the first n_j approximations are close to the correct value. This accuracy is determined by the ability of n_j elements to describe the corresponding mode shape correctly. Geradin and Rixen (*14*) also observe that the approximations are upper bounds of correct value.

For constant spin, the trim motion in response to the spinning bent missile forces can be obtained by assuming a solution of the form

$$q_n = q_{nT} e^{i\dot{\phi} t} . \tag{55}$$

The response parameters, q_{nT}, vary with particular values of the constant spin and are solutions of a set of n_t linear inhomogeneous algebraic equations,

$$\sum_{n=1}^{n_t} B_{mn} q_{nT} = t_m , \tag{56}$$

where $B_{mn} = -\dot{\phi}^2 \left(R_{mn} + S^*_{mn} \right) + i\dot{\phi} \left(S_{mn} + T^*_{mn} \right) + T_{mn}$.

In reference (*12*), both these special solutions were computed from iterative solutions of a second-order differential equation specified by special boundary conditions. The FEM approach obtains the same results and more by much simpler matrix operations.

7. Quadratic Roll Equation

The linear roll equation (equation 26) was derived from a kinetic energy function, which neglected cubic terms in q_{1y}, q_{1z}, q_{2y}, q_{2z}, q_{bny}, and q_{bnz}. In order to derive the quadratic roll equation, cubic terms involving ϕ and $\dot{\phi}$ must be retained. The resulting roll equation is the same as that derived in reference (*12*) from Newtonian mechanics,

$$I_x \ddot{\phi} + \mathrm{Re}\left\{ md^2 \left(\dot{J}_7 - i\dot{q}_2 \overline{J}_6 + iq_2 \overline{J}_8 \right) - iF\overline{\delta}_c d \right\} = M_x , \tag{57}$$

where $J_7(t)$ is defined in appendix F.

The aerodynamic roll moment is the X-component of the aerodynamic moment about the center of the central disk. The linear roll moment coefficient for a rigid finned projectile is usually expressed in terms of a roll-damping coefficient and a steady state spin,

$$\left(C_{\ell}\right)_{\text{linear}} = C_{\ell p}\left(\dot{\phi} - p_{ss}\right)\ \left(d/V\right). \tag{58}$$

The steady state spin is usually determined by a differential canting of the fins caused either intentionally by the designer or unintentionally by damage to the projectile.

The roll moment of one of the projectile's thin disks is the sum of the linear roll moment it has as part of a projectile and the quadratic roll moment induced by the transverse aerodynamic force acting on its lateral displacement relative to the center of the central disk. If we retain only the dominant c_{f1} term in equation 20, the quadratic roll moment has the form

$$\begin{aligned}\left(\ dM_x\right)_{\text{quadratic}} &= \left[\left(dF_z\right)\ \delta_{Ey} - \left(dF_y\right)\ \delta_{Ez}\right] \\ &= \left(g_1 d\right)\ c_{f1}\,\text{Re}\ \left\{\ i\left[\left(q_1 - \Gamma - \Gamma_{BF}e^{i\phi}\right) + \left(\dot{\delta}_E - x\dot{q}_1\right)\ \left(d/V\right)\right]\ \overline{\delta}_E\right\} dx\,. \end{aligned} \tag{59}$$

The total aerodynamic roll moment acting on the projectile, therefore,

$$M_x = \left(g_1 d\right)\ \left[\ \left(C_{\ell}\right)_{\text{linear}} + \text{Re}\left\{\ Q_A\left(t\right) - i g_1^{-1} F\overline{\delta}_c\right\}\ \right], \tag{60}$$

where $Q_A\left(t\right) = i\int_{x_0}^{x_3} c_{f1}\left[\left(q_1 - \Gamma - \Gamma_{BF}e^{i\phi}\right) + \left(\dot{\delta}_E - x\dot{q}_1\right)\ \left(d/V\right)\right]\ \left(\overline{\delta}_E - \overline{\delta}_c\right)\ dx\,.$

The nonlinear roll moment from equation 60 can be placed in the spin equation 57 to yield:

$$I_X\ddot{\phi} + \text{Re}\left\{md^2\left(Q_D - i\dot{q}_2\overline{J}_6 + iq_2\overline{J}_8\right) - g_1 d\,Q_A\right\} = g_1 d\left(C_{\ell}\right)_{\text{linear}}, \tag{61}$$

where the quadratic terms $I_X.Q_D$ are defined in appendix F.

For trim motion, $\ddot{\phi} = \text{Re}\ \left\{\ Q_D\right\} = 0,\ \dot{q}_2 = i\dot{\phi}q_{2T}e^{i\dot{\phi}t}$ and equation 61 become a simple equality of two functions of p.

$$f_2\left(\dot{\phi}\right) = f_1\left(\dot{\phi}\right), \tag{62}$$

where $f_1 = \dot{\phi} - p_{ss}$, $f_2 = \text{-R}\left\{Q_{AT} - \left(q_{2T}md/g_1\right)\left(\dot{\phi}\overline{J}_{6T} + i\overline{J}_{8T}\right)\right\}\left(C_{lp}d/V\right)^{-1}$, and

$Q_{AT} = i\int_{x_0}^{x_3} c_{f1}\left[\left(q_{1T} - \Gamma_T - \Gamma_{BF}\right) + i\left(\delta_{ET} - xq_{1T}\right)\left(\dot{\phi}d/V\right)\right]\overline{\delta}_T dx\,.$

δ_{ET}, Γ_T are computed from the solution to equation 56 and J_{6T}, J_{8T} are J_6, J_8 evaluated for δ_{ET}, Γ_T. For moderate spin Q_{AT} is the dominant part of f_2. Equilibrium values of spin are determined by the intersection of these two curves. Lockin occurs at stable equilibrium spin.

Spin lockin can only occur when the missile has some rigid asymmetry such as that described by δ_{EB} or Γ_{BF}. For a rigid missile δ_{ET} and Γ_T are δ_{EB} and Γ_B. q_{1T} is a function of spin which has a large resonant amplitude when spin is near ω_R. For an elastic missile $q_{1T}, \delta_{ET}, \Gamma_T$ are all functions of spin and have large resonant amplitudes when spin is near $\dot{\phi}_{2k-1}$ or near $\dot{\phi}_{2k}$ for negative spin.

8. Numerical Results

In reference (*12*), calculations were made for a 20-cal. fin-stabilized rod, flying at 6000 ft/s. The finned missile has a 1-cal. nose extension and a 1-cal. fin extension (figure 3). The mass and aerodynamic parameters for the finned missile are given in appendix H. The bent rod will be described by a pair of quartic curves.

$$\begin{aligned} \delta_{EB} &= d_{11}x^2 + d_{21}x^4 \qquad -10 \le x \le 0 \\ &= d_{12}x^2 + d_{22}x^4 \qquad 0 \le x \le 10. \end{aligned} \tag{63}$$

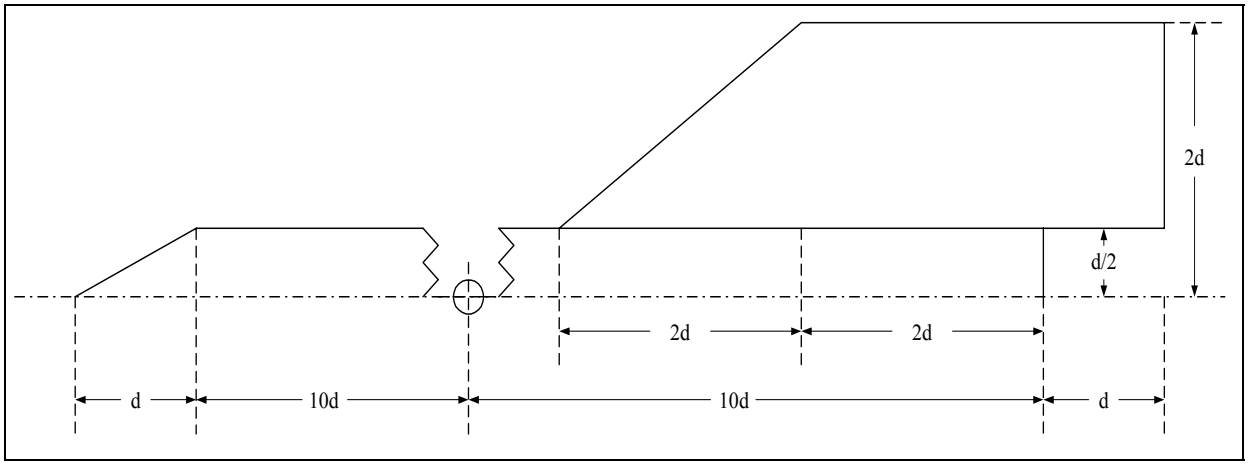

Figure 3. Sketch of finned missile.

The rear of the rod is undeformed ($d_{11} = d_{21} = 0$), and the values of d_{12}, d_{22} are given in appendix G. Two values of Γ_{BF} will be considered. These are unbent fins and the rear 1 cal. of fins bent uniformly to an angle of 0.02 radians.

A measure of the flight flexibility of a missile is the ratio of the first elastic frequency to the rigid missile aerodynamic frequency, $\sigma \equiv \omega_1/\omega_R$. Calculations of $\dot{\phi}_1$ vs. σ have been made for the 1-, 3-, 5-, and 7-element rod. The results for all but the 1-element rod are practically identical, and the curve for a 3-element rod is given in figure 4. At $\sigma = 5$, the aerodynamic frequency is 60% of the rigid missile aerodynamic frequency; and even at $\sigma = 10$, it is 10% less than the rigid missile aerodynamic frequency.

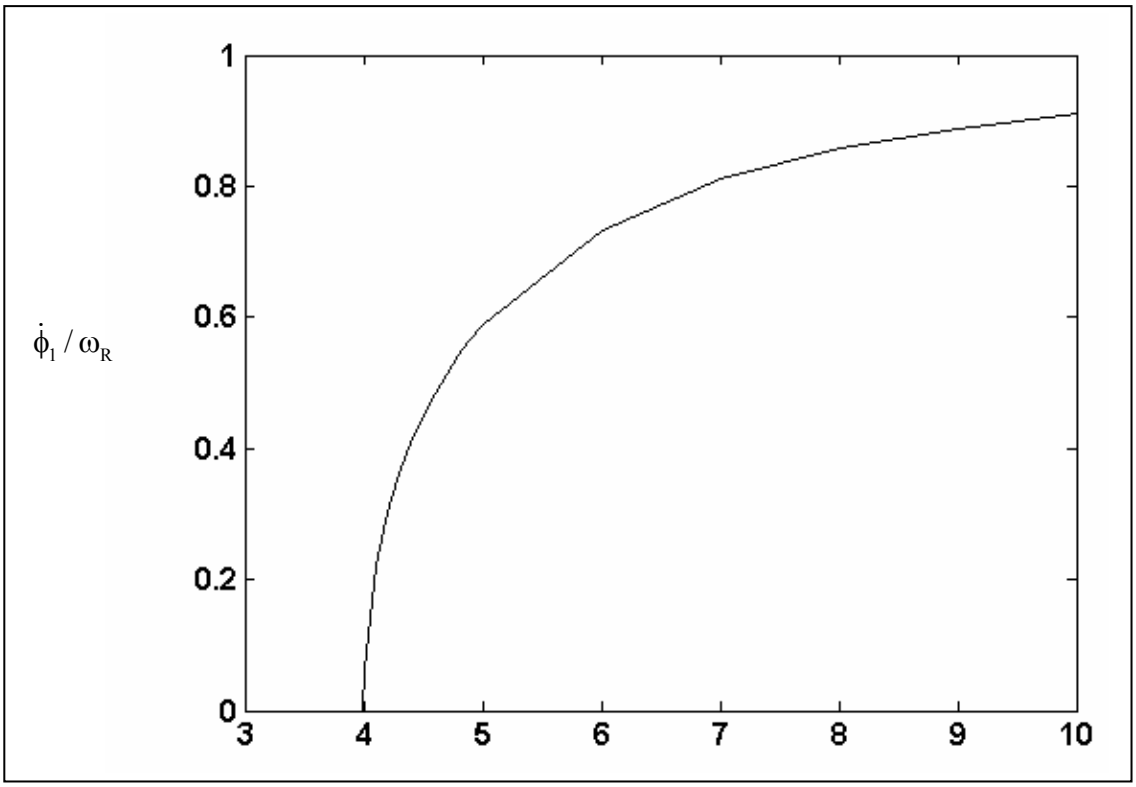

Figure 4. $\dot{\phi}_1 / \omega_R$ vs. σ for finned missile.

The first six positive frequencies and their damping rates for $\sigma = 5$ have been calculated for a 1-, 3-, 5-, and 7-element rod. These results, together with calculations from the theory of reference (*12*), are tabulated in table 1. We identify frequencies which differ from the reference (*12*) value by >10% as poor values and mark them with x's. Thus the 1-element rod yields one moderately good result while the 3-element and 5-element rods yield three and five good results, respectively. For this elastic problem, $n_j - 1$, elastic frequencies are well calculated. For zero spin, the negative frequencies are the negatives of the positive frequencies.

Because the 3-element rod predicts the lower three frequencies quite well, all of the calculations given in this report are based on a 3-element rod. Most of these have been repeated for a 5-element rod, and almost identical results have been obtained.

In figure 5, f_2 for $\sigma = 5, \Gamma_{BF} = 0$ is plotted vs. $\dot{\phi}/\omega_R$ for spin near the first elastic frequency. Large resonance values occur at $\dot{\phi}/\omega_R \cong 5.1$ and an f_1 line for $p_{ss} = 6.0\omega_R$ is also shown. This f_1 line has three intersections with the f_2 curve, which are values of equilibrium spin. The intersection near p_{ss}/ω_R is denoted as p_{ss}/ω_R, while the other two are p_{1e}/ω_R, p_{2e}/ω_R, and all their numerical values are given in table 2.

Table 1. Transient frequencies and damping rates.

$\sigma = 5$ $\dot{\phi} = 0$			
Code	**k**	$\dot{\phi}_k / \omega_R$	λ_k / ω_R
1 element	1	0.645	–0.0530
3 element	1	0.612	–0.0528
5 element	1	0.613	–0.0528
7 element	1	0.613	–0.0528
reference (*12*)	1	0.614	–0.0529
1 element	3	6.146×	–0.0855
3 element	3	5.194	–0.0724
5 element	3	5.181	–0.0718
7 element	3	5.180	–0.0717
reference (*12*)	3	5.184	–0.0717
1 element	5	20.31×	–0.0644
3 element	5	13.81	–0.0518
5 element	5	13.79	–0.0523
7 element	5	13.76	–0.0518
reference (*12*)	5	13.74	–0.0506
1 element	7	—	—
3 element	7	30.00×	–0.1018
5 element	7	26.97	–0.0914
7 element	7	26.79	–0.0881
reference (*12*)	7	26.69	–0.0825
1 element	9	—	—
3 element	9	53.37×	–0.2060
5 element	9	44.28	–0.1389
7 element	9	44.18	–0.1462
reference (*12*)	9	43.84	–0.1427
1 element	11	—	—
3 element	11	100.44×	–0.4708
5 element	11	72.19×	–0.1309
7 element	11	65.88	–0.1256
reference (*12*)	11	64.49	–0.1202

In figure 6, spin histories are plotted for all initial conditions equal to zero except $\dot{\phi}_0 = 0, 5.4\omega_R$. For low values of initial spin, lockin occurs at the first elastic frequency, p_{1e}, and large strains result. For larger values of initial spin, lockin occurs at p_{sse}. This behavior was predicted by the simple three-body theory of reference (*11*).

It is very unlikely that sufficient fin damage occurs to produce a p_{ss} in excess of five times ω_R. Because it is much more likely that a p_{ss} near ω_R can be produced, the observed inelastic deformation is probably caused by lockin at the aerodynamic frequency, and this case is considered in detail in the following section.

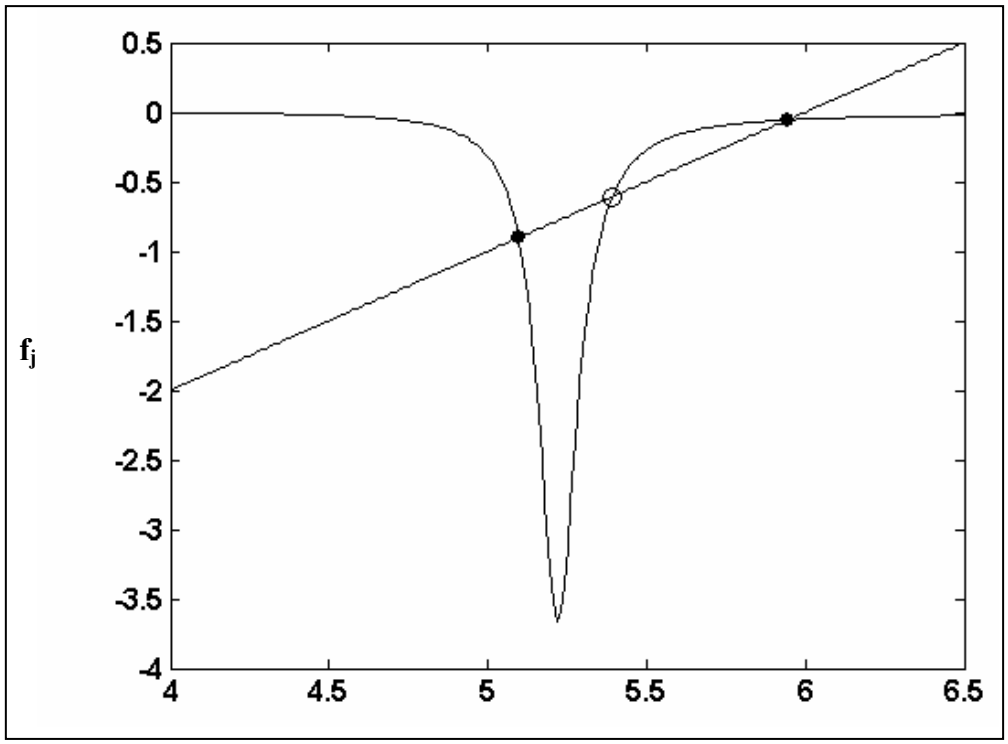

Figure 5. f_j vs. $\dot{\phi}/\omega_R$ for $\Gamma_{BF} = 0,\ \sigma = 5, p_{ss} = 6\omega_R$.

Table 2. Equilibrium spin rates.

$\sigma = 5$			
Γ_{BF}	**0**	**0**	**0.02**
p_{ss}/ω_R	6.000	0.800	0.400
p_{sse}/ω_R	5.944	0.788	0.429
p_{1e}/ω_R	5.097	0.590	0.564
p_{ss}/ω_R	5.393	0.647	0.627

In figure 7, f_2 is plotted for spins near the aerodynamic frequency, and f_1 is shown for $p_{ss} = 0.8\omega_R$. The three intersection points are given in table 2. Spin histories are plotted in figure 8 for zero initial conditions except for $\dot{\psi}_0 = 0, -3\ s^{-1}$. Here, we see that p_{sse} spin-yaw lockin occurs for zero initial angular velocity, and p_{1e} spin-yaw lockin for an initial yaw rate of –3 s^{-1}. The angular motion in body-fixed coordinates is plotted in figure 9. For lockin at p_{sse}, the motion is smaller than 0.09 rad, while for lockin at p_{1e}, it is as large as 0.15 rad. The motion of the forward end of the rod in body-fixed coordinates is given in figure 10. Motion for p_{sse} lockin is <0.17 (0.7 in), and after 1 s, it is never >0.09 (0.4 in). For p_{1e} lockin, it exceeds 0.28 (1.2 in).

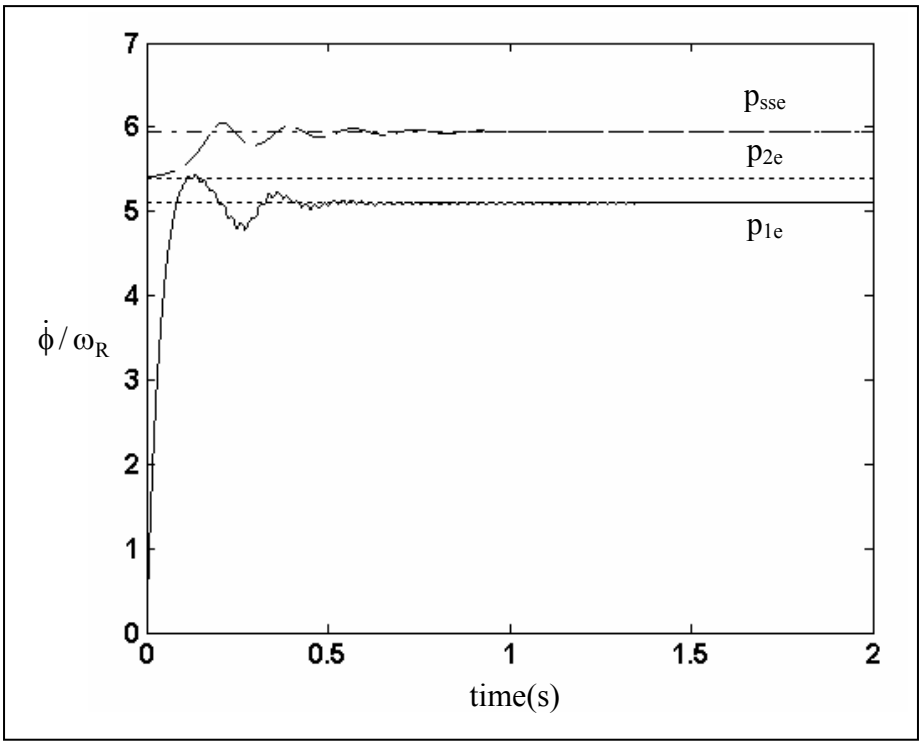

Figure 6. $\dot{\phi}/\omega_R$ vs. time for $\Gamma_{BF} = 0,\ \sigma = 5,\ p_{ss} = 6.0\omega_R,\ \dot{\phi}_0/\omega_R = 0, 5.4$.

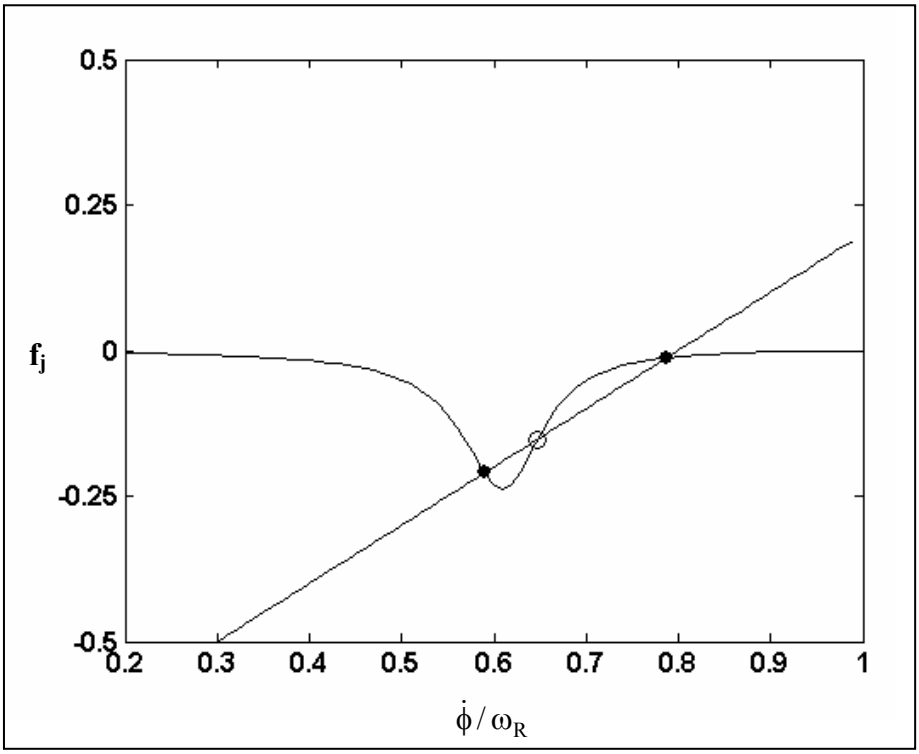

Figure 7. f_j vs. $\dot{\phi}/\omega_R$ for $\Gamma_{BF} = 0,\ \sigma = 5,\ p_{ss} = 0.8\omega_R$.

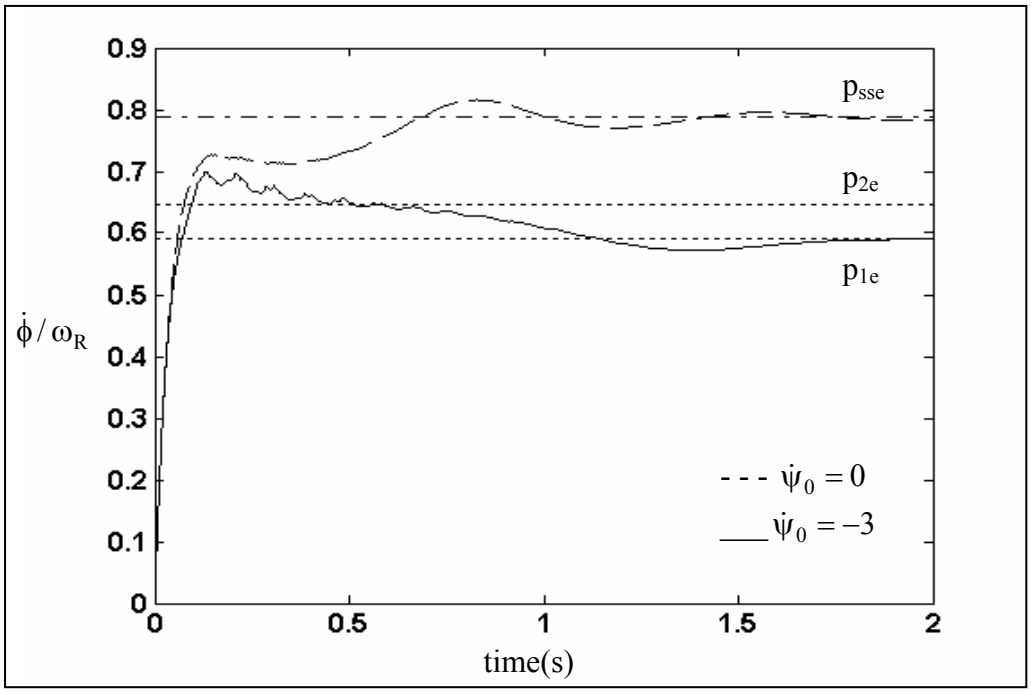

Figure 8. $\dot{\phi}/\omega_R$ vs. time for $\Gamma_{BF} = 0,\ \sigma = 5,\ p_{ss} = 0.8\omega_R,\ \dot{\psi}_0 = 0, -3\ s^{-1}$.

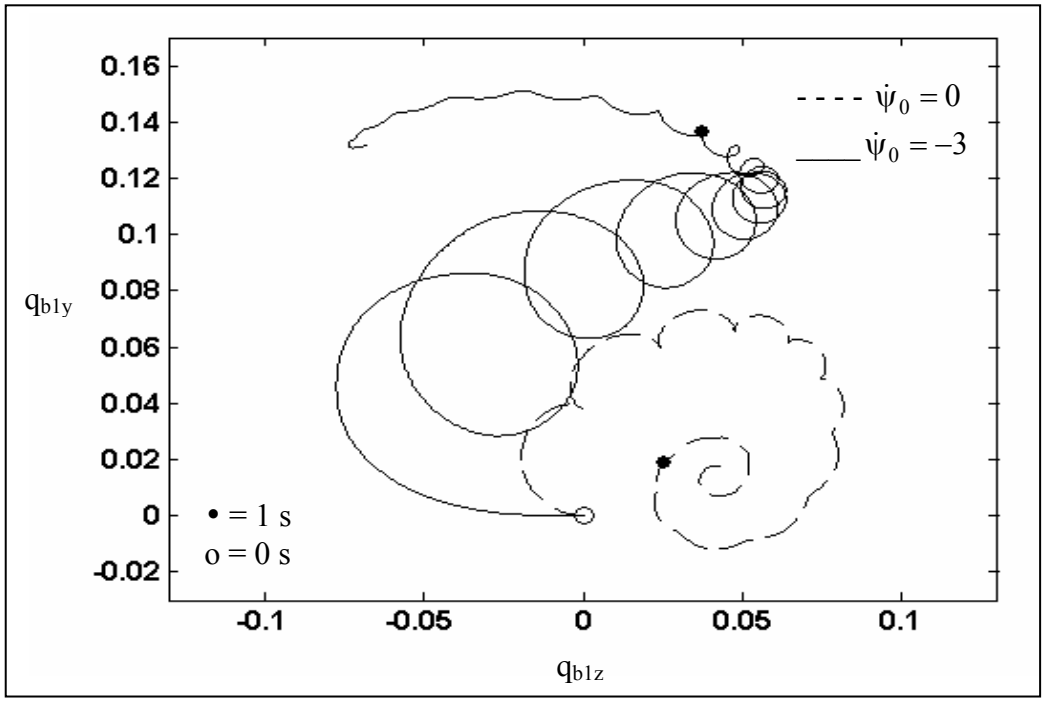

Figure 9. Angular motion (q_{b1y} vs. q_{b1z}) for $\Gamma_{BF} = 0,\ \sigma = 5,\ p_{ss} = 0.8\omega_R,\ \dot{\psi}_0 = 0,\ -3\ s^{-1}$.

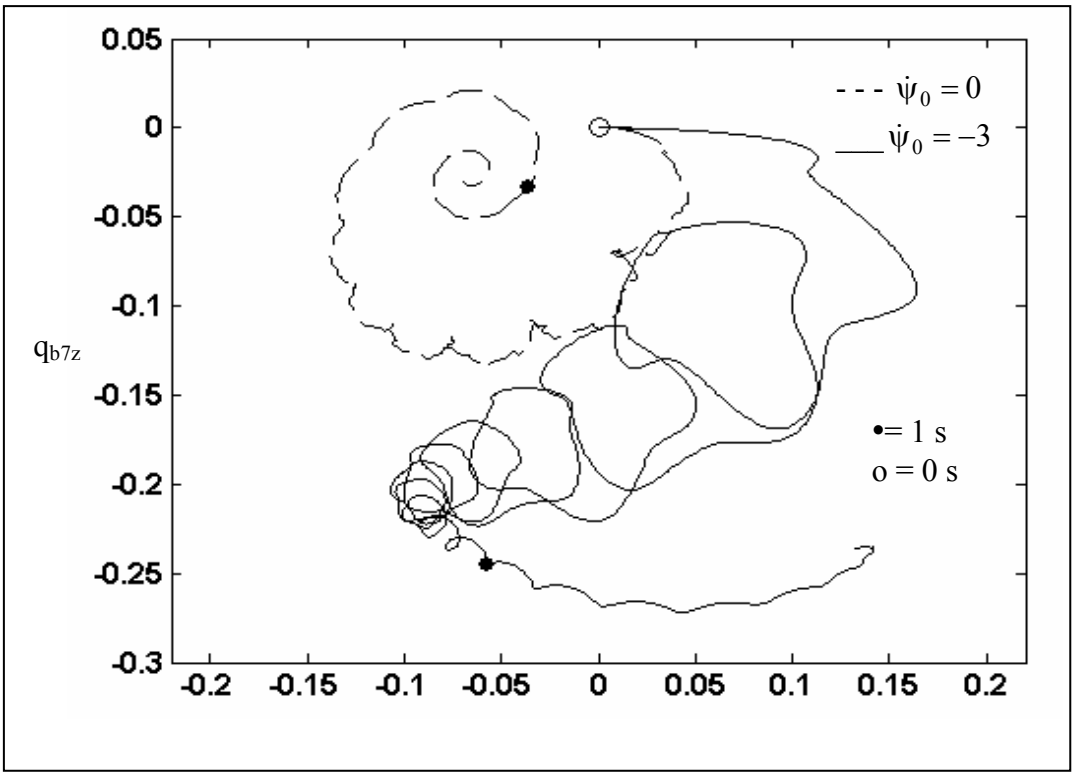

Figure 10. Rod forward tip motion (q_{b7y} vs. q_{b7z}) for $\Gamma_{BF} = 0$, $\sigma = 5$, $p_{ss} = 0.8\omega_R$, $\dot{\psi}_0 = 0, -3\ s^{-1}$.

The maximum strain on the rod is located on the rod's surface at its center. In terms of 3-element parameters, the maximum strain is

$$\varepsilon_M = (1/2)\left|\frac{\partial^2 \delta_E(0)}{\partial x^2}\right| = L_e^{-2}\left|12q_5 + 2L_e q_6\right|. \tag{64}$$

The time history of the maximum strain is plotted in figure 11 for $\dot{\psi}_0 = 0,\ -3\ s^{-1}$. For most metals, yield occurs for maximum strains in excess of 0.0015, and we see that yield does occur for resonance lockin.

The two regions of the initial angular rate plane, i.e., the $\dot{\psi}_0 - \dot{\theta}_0$ plane, which induces either lockin, can be determined by a number of trial and error calculations, and the boundary curve between these regions is shown in figure 12. Initial conditions outside this curve will cause resonance lockin while conditions inside it induce p_{sse} lockin.

For $\Gamma_{BF} = 0$, the first resonance peak of the f_2 curve is negative, and p_{ss} must be greater than the aerodynamic frequency for three intersections to occur.

As is shown in figure 13, bent fins corresponding to $\Gamma_{BF} = 0.02\ -11 \le x \le -10$ will produce a positive peak in the f_2 curve and a p_{ss} less than the aerodynamic frequency can produce resonance lockin. The plots corresponding to figures 8–12 are given by figures 13–19.

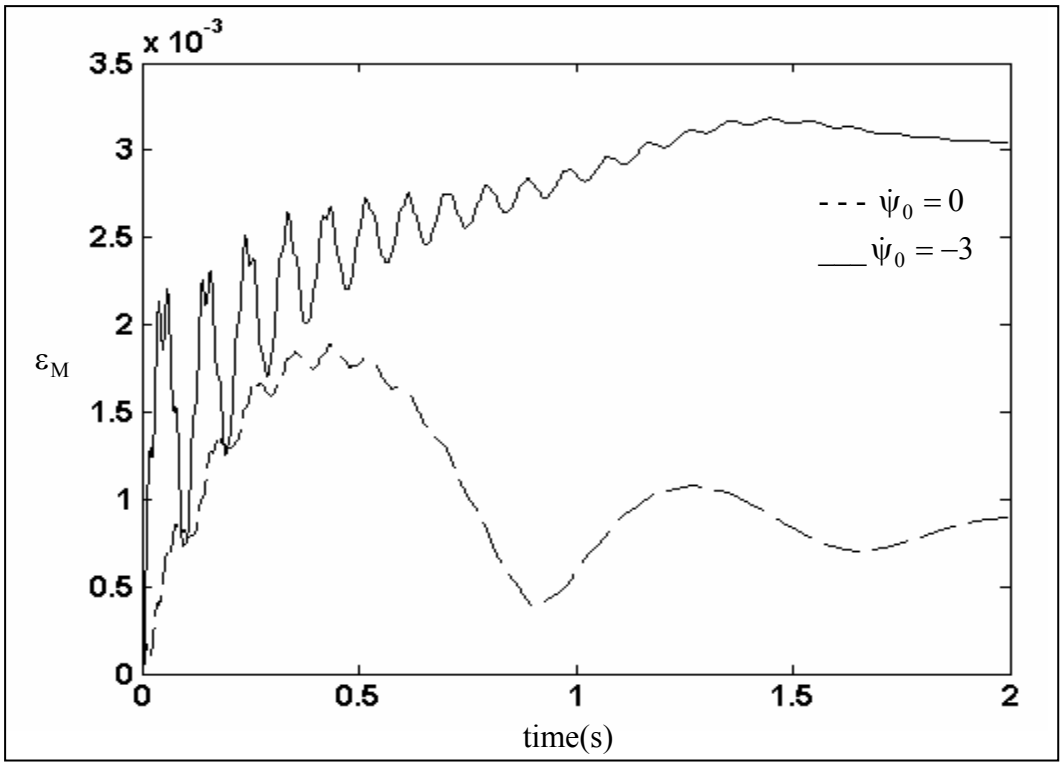

Figure 11. Maximum strain (ε_M) for $\Gamma_{BF} = 0$, $\sigma = 5$, $p_{ss} = 0.8\omega_R$, $\dot{\psi}_0 = 0, -3$ s^{-1}.

9. Summary

The application of FEM to the calculation of the motion of a pitching, yawing, and flexing missile has resulted in the construction of a family of linear differential equations.

Computer codes have been developed for 1, 3, 5, and 7 elements and used to obtain the first four elastic frequencies. The 3-element code has given excellent values of the first two elastic frequencies. The 5-element and 7-element codes provide equally good values for the first four elastic frequencies.

Integration of these differential equations has demonstrated resonant spin lockin at the aerodynamic frequency and the first elastic frequency. Lockin can occur near the design steady state spin or near resonance with a transient frequency. Calculations have identified regions of a yaw rate-pitch rate plane that determine which lockin will occur.

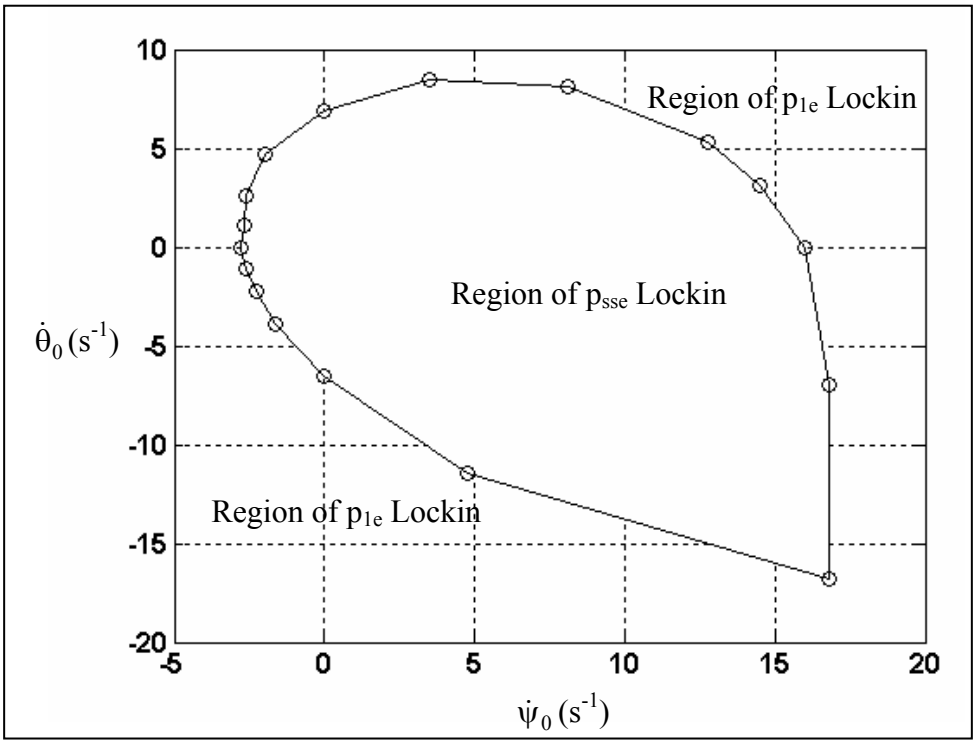

Figure 12. $\dot{\psi}_0$ vs. $\dot{\theta}_0$ showing regions of p_{sse}, p_{1e} lockin $\Gamma_{BF} = 0, \sigma = 5, p_{ss} = 0.8\omega_R$.

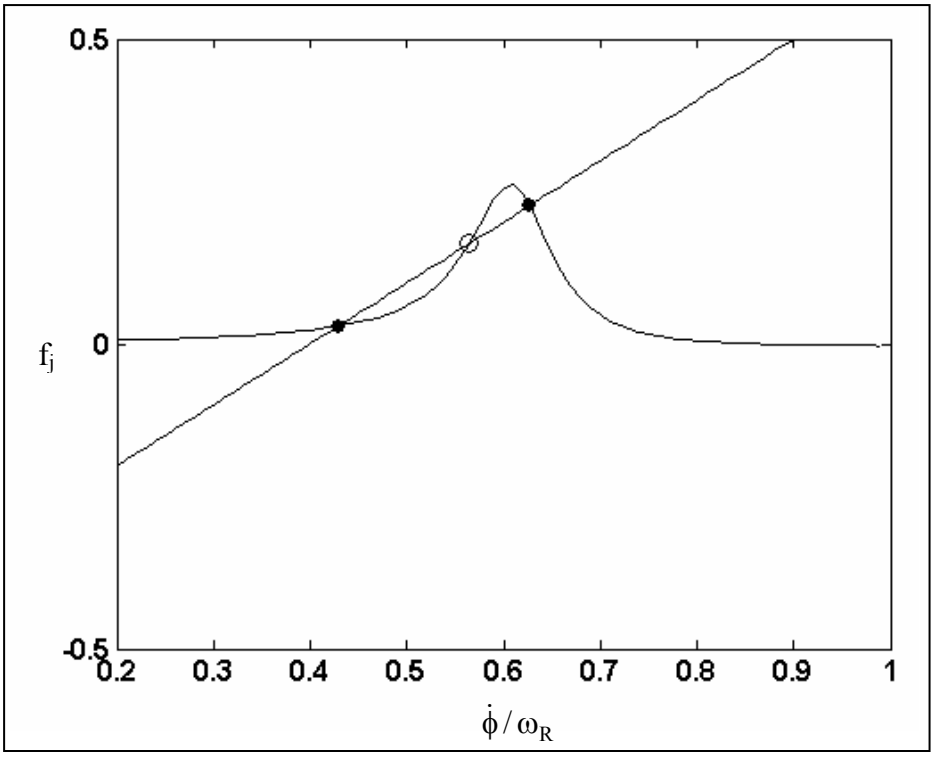

Figure 13. f_j vs. $\dot{\phi}/\omega_R$ for $\Gamma_{BF} = 0.02,\ \sigma = 5,\ p_{ss} = 0.4\omega_R$.

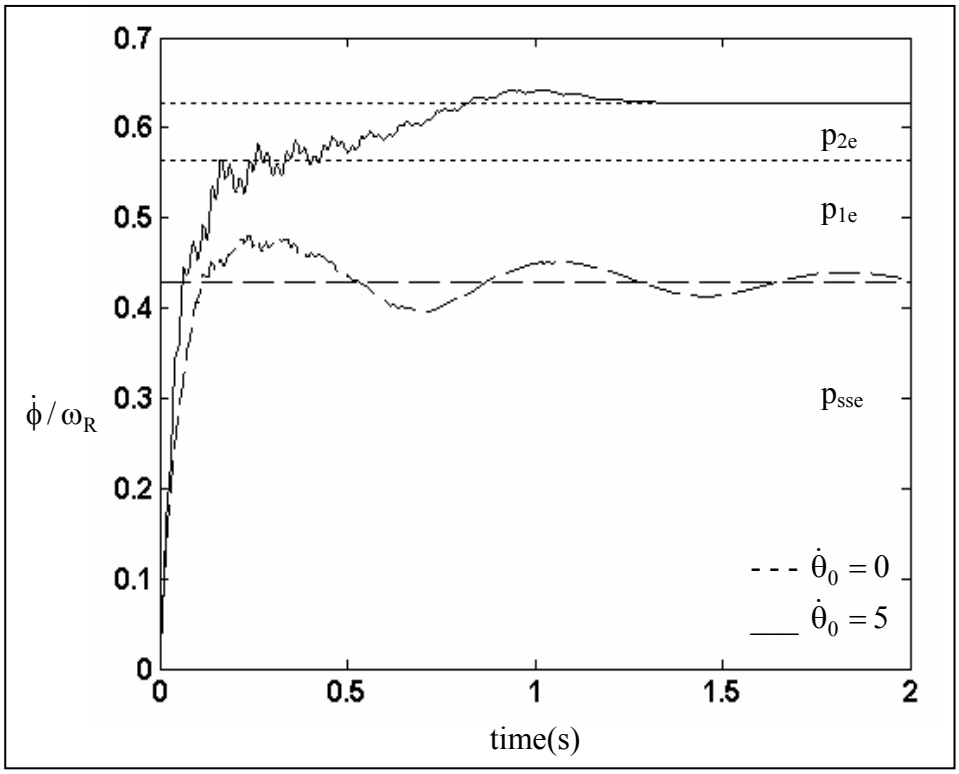

Figure 14. $\dot{\phi}/\omega_R$ vs. time for $\Gamma_{BF} = 0.02,\ \sigma = 5,\ p_{ss} = 0.4\omega_R,\ \dot{\theta}_0 = 0,\ 5\ s^{-1}$.

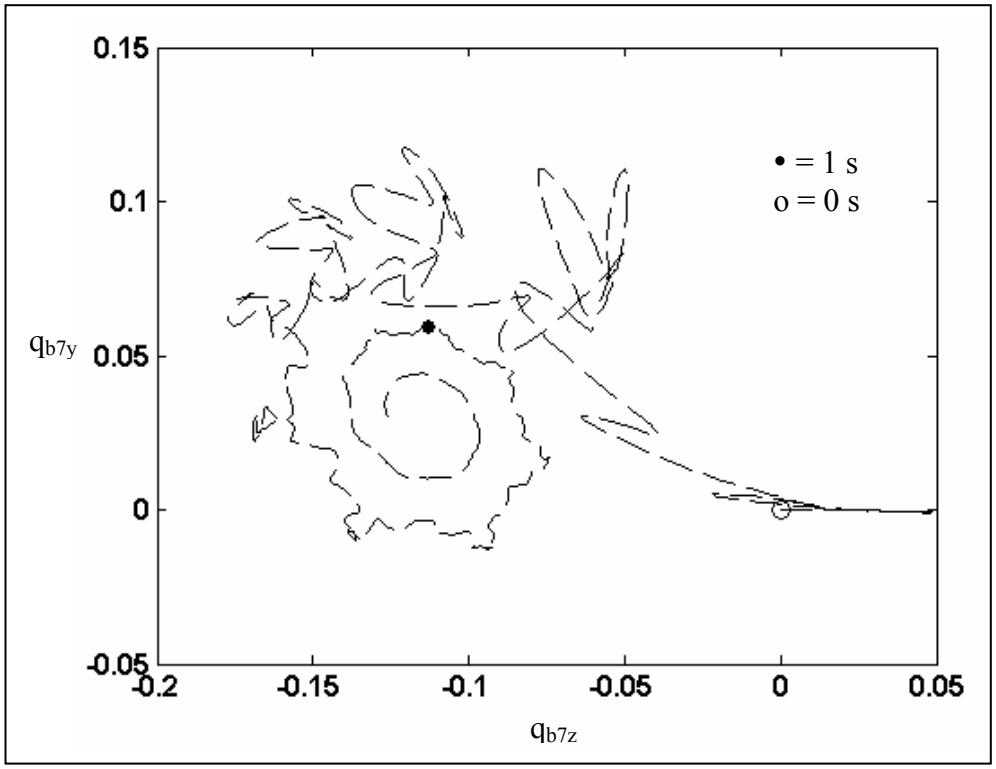

Figure 15. Angular motion (q_{b1y} vs. q_{b1z}) for $\Gamma_{BF} = 0.02,\ \sigma = 5,\ p_{ss} = 0.4\omega_R,\ \dot{\theta}_0 = 0,\ 5\ s^{-1}$.

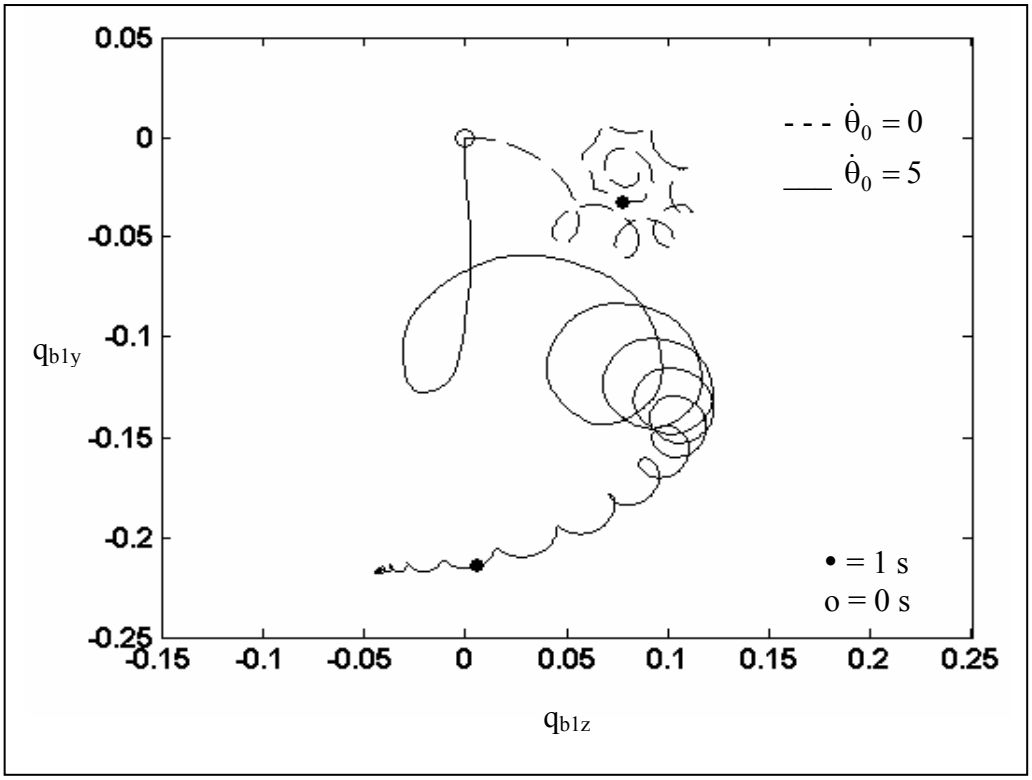

Figure 16. Rod forward tip motion (q_{b7y} vs. q_{b7z}) for $\Gamma_{BF} = 0.02,\ \sigma = 5,\ p_{ss} = 0.4\omega_R,\ \dot{\theta}_0 = 0\ s^{-1}$.

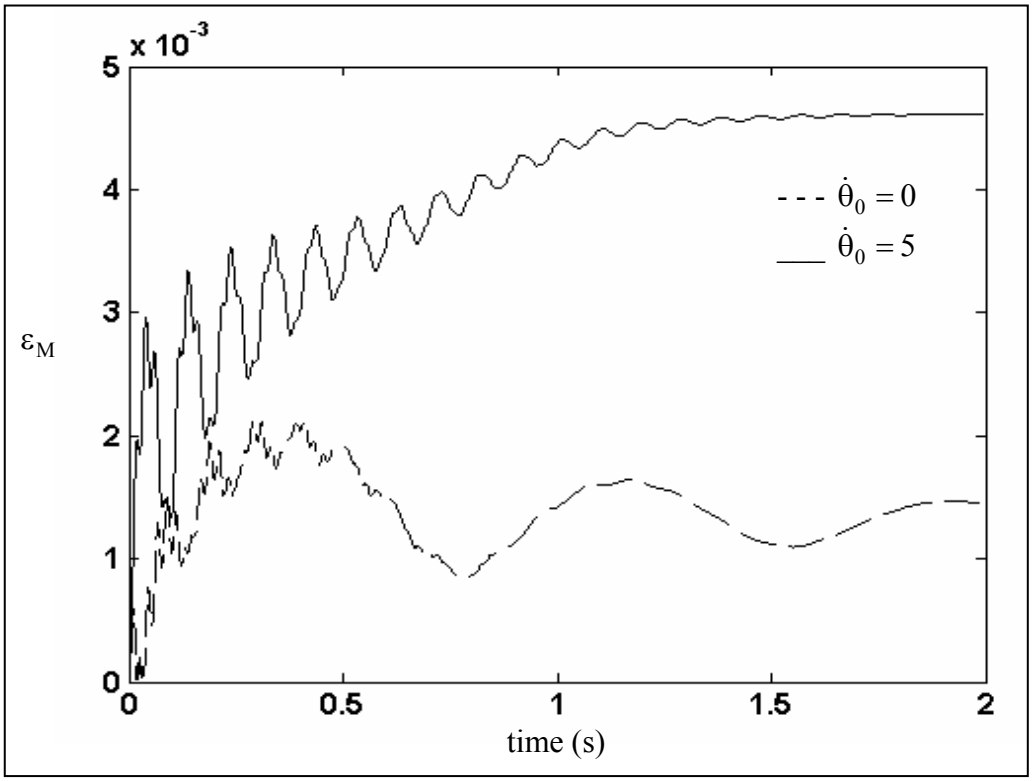

Figure 17. Rod forward tip motion (q_{b7y} vs. q_{b7z}) for $\Gamma_{BF} = 0.02,\ \sigma = 5,\ p_{ss} = 0.4\omega_R,\ \dot{\theta}_0 = 5\ s^{-1}$.

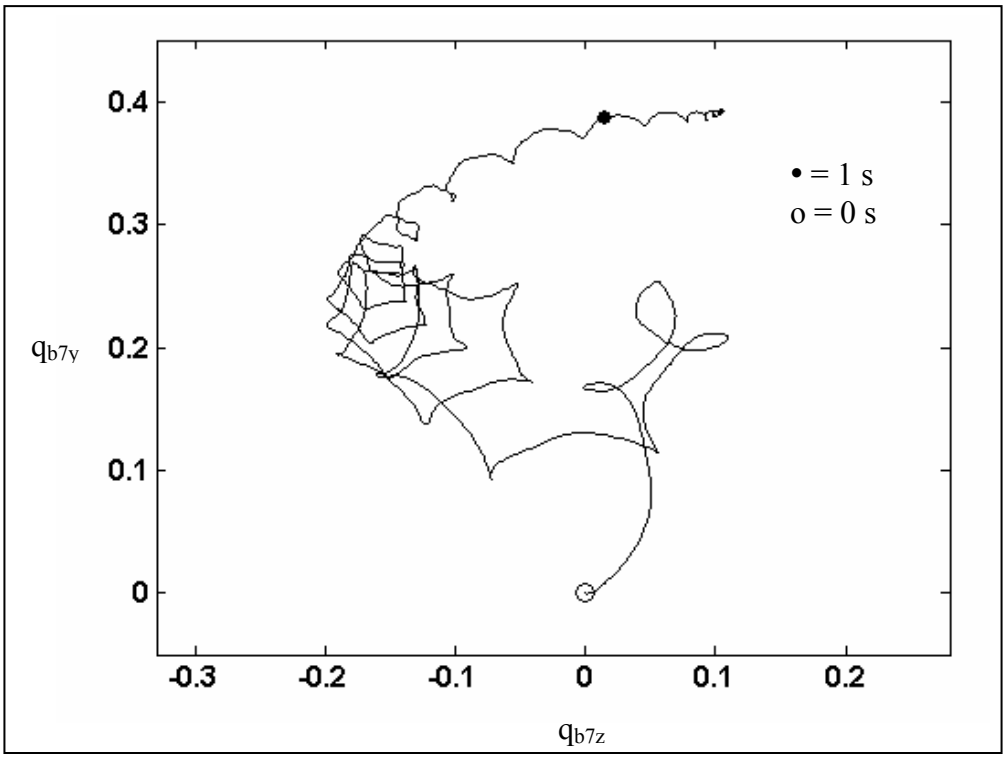

Figure 18. Maximum strain (ε_M) for $\Gamma_{BF} = 0.02,\ \sigma = 5,\ p_{ss} = 0.4\omega_R,\ \dot{\theta}_0 = 0,\ 5\ s^{-1}$.

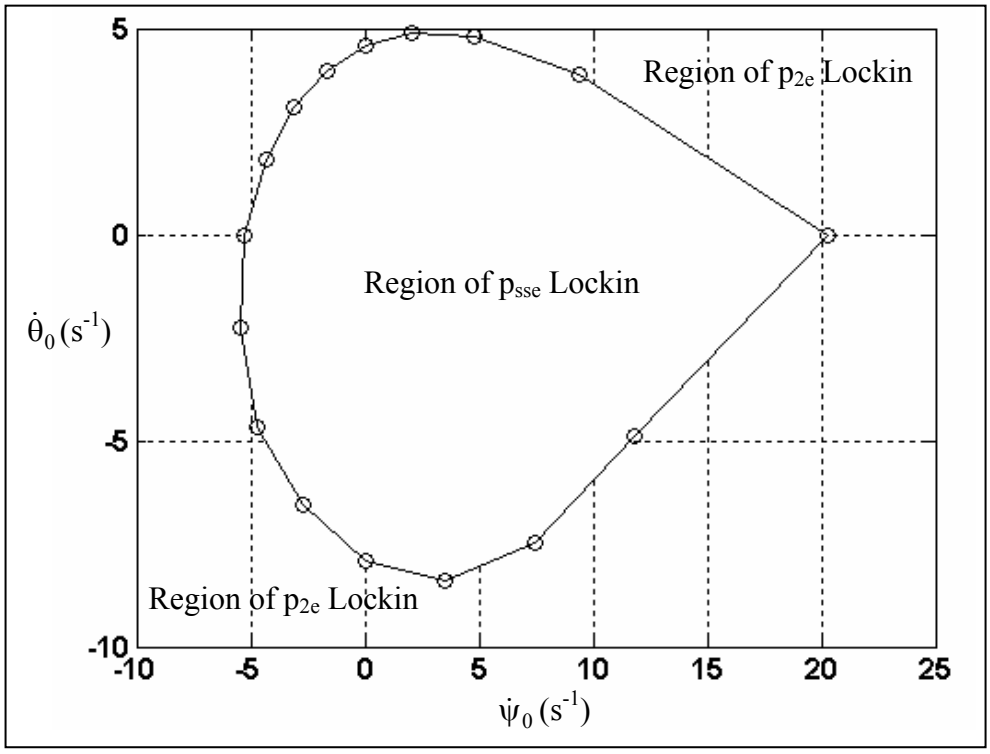

Figure 19. $\dot{\psi}_0$ vs. $\dot{\theta}_0$ showing regions of p_{sse}, p_{2e} lockin $\Gamma_{BF} = 0.02, \sigma = 5, p_{ss} = 0.4\omega_R$.

10. References

1. Mikhail, A. G. In-Flight Flexure and Spin Lock-in for Anti-Tank Kinetic Energy Projectiles. *Journal of Spacecraft and Rockets* **1996**, *33*, 657–664.

2. Guidos, B. J.; Garner, J. M.; Newill, J. F.; Livecchia, C. D. *Measured In-Flight Rod Flexure of a 120-mm M829E3 Kinetic Energy (KE) Projectile Steel Model*; ARL-TR-2820; U.S. Army Research Laboratory: Aberdeen Proving Ground, MD, 2002.

3. Peppitone, T. R.; Jacobson, J. D. Resonant Behavior of a Symmetric Missile Having Roll Orientation-Dependent Aerodynamics. *Journal of Guidance and Control* **1978**, *1*, 335–339.

4. Grover, L. S. Effects on Roll Rate of Mass and Aerodynamic Asymmetries On Ballistic Re-Entry Bodies. *Journal of Spacecraft and Rockets* **1965**, *2*, 220–225.

5. Price, D. A., Jr. Sources, Mechanisms, and Control of Roll Resonance Phenomena for Sounding Rockets. *Journal of Spacecraft and Rockets* **1967**, *4*, 1516–1525.

6. Price, D. A., Jr.; Ericsson, L. E. A New Treatment of Roll-Pitch Coupling for Ballistic Re-Entry Bodies. *AIAA Journal* **1970**, *80*, 1608–1615.

7. Murphy, C. H. Some Special Cases of Spin-Yaw Lock-In. *Journal of Guidance, Control, and Dynamics* **1989**, *12*, 771–776.

8. Platus, D. H. Aeroelastic Stability of Slender, Spinning Missiles. *Journal of Guidance, Control, and Dynamics* **1992**, *15*, 144–151.

9. Legner, H. H.; Lo, E. Y.; Reinecke, W. G. On the Trajectory of Hypersonic Projectiles Undergoing Geometry Changes. *AIAA Aerospace Sciences Meeting*, Reno, NV, 10–13 January 1994; AIAA 94-0719.

10. Heddadj, S.; Cayzac, R.; Renard, J. Aeroelasticity of High L/D Supersonic Bodies: Theoretical and Numerical Approach. *AIAA Aerospace Sciences Meeting*, Reno, NV, 10–13 January 2000; AIAA 2000-0390.

11. Murphy, C. H.; Mermagen, W. H. Flight Mechanics of an Elastic Symmetric Projectile. *Journal of Guidance, Control, and Dynamics* **2001**, *24*, 1125–1132.

12. Murphy, C. H.; Mermagen, W. H. Flight Motion of a Continuously Elastic Finned Missile. *Journal of Guidance, Control, and Dynamics* **2003**, *26*, 89–98.

13. Murphy, C. H.; Mermagen, W. H. *Flight Motion of a Continuously Elastic Finned Missile*; ARL-TR-2754; U.S. Army Research Laboratory: Aberdeen Proving Ground, MD, 2002.

14. Geradin, M.; Rixen, D. *Mechanical Vibrations: Theory and Applications to Structural Dynamics*; John Wiley & Sons: New York, 1994.

15. Murphy, C. H. *Free Flight Motion of Symmetric Missiles*; BRL-TR-1216; U.S. Army Ballistics Research Laboratory: Aberdeen Proving Ground, MD, 1963.

16. DeSilver, C. W. *Vibration Fundamentals and Practice*; CRC Press: New York, 2000; p 351.

Appendix A. Integrals

A.1 Aerodynamic Terms

$$c_1 = C_{N\alpha} = \int_{x_0}^{x_3} c_{f1}dx \qquad c_3 = C_{M\alpha} = \int_{x_0}^{x_3} c_{f1}xdx$$

$$c_2 = C_{Nq} + C_{N\dot{\alpha}} = \int_{x_0}^{x_3} c_{f3}dx \qquad c_4 = C_{Mq} + C_{M\dot{\alpha}} = \int_{x_0}^{x_3} c_{f3}xdx$$

$$C_{NBF} = \int_{x_0}^{x_3} c_{FB}\Gamma_{BF}dx \qquad C_{MBF} = \int_{x_0}^{x_3} c_{BF}\Gamma_{BF}xdx$$

$$c_{f3} = 2c_{f2} - xc_{f1} \qquad c_{BF} = c_{f1} + \left(\dot{\phi}d/V\right)\, c_{f2}. \qquad \text{(A-1)}$$

A.2 Boundary Terms

$$I_1 = \int_{x_0}^{x_1} c_{f1}dx \qquad I_2 = \int_{x_2}^{x_3} c_{f1}dx$$

$$I_3 = \int_{x_0}^{x_1} \left(x - x_1\right)c_{f1}dx \qquad I_4 = \int_{x_2}^{x_3} \left(x - x_2\right)\, c_{f1}dx$$

$$I_5 = \int_{x_0}^{x_1} c_{f2}dx \qquad I_6 = \int_{x_2}^{x_3} c_{f2}dx$$

$$I_7 = \int_{x_0}^{x_1} \left(x - x_1\right)c_{f2}dx \qquad I_8 = \int_{x_2}^{x_3} \left(x - x_2\right)\, c_{f2}dx$$

$$I_9 = \int_{x_0}^{x_1} \left(x - x_1\right)^2 c_{f1}dx \qquad I_{10} = \int_{x_2}^{x_3} \left(x - x_2\right)^2 c_{f1}dx$$

$$I_{11} = 2I_5 - I_3 - x_1 I_1 \qquad I_{12} = 2I_6 - I_4 - x_2 I_2$$

$$I_{13} = 2I_7 - I_9 - x_1 I_3 \qquad I_{14} = 2I_8 - I_{10} - x_2 I_4$$

$$I_{1D} = \int_{x_0}^{x_1} c_D dx + C_{Dbp} \qquad I_{2D} = \int_{x_2}^{x_3} c_D dx$$

$$I_{3D} = \int_{x_0}^{x_1} \left(x - x_1\right)c_D dx \qquad I_{4D} = \int_{x_2}^{x_3} \left(x - x_2\right)\, c_D dx$$

$$I_{1BF} = \int_{x_0}^{x_1} c_{BF}\Gamma_{BF}dx \qquad I_{3BF} = \int_{x_0}^{x_1} \left(x - x_1\right)\, c_{BF}\Gamma_{BF}dx$$

$$I_{5BF} = \int_{x_0}^{x_1} c_{f2}\Gamma_{BF}dx \qquad I_{7BF} = \int_{x_0}^{x_1} \left(x - x_1\right)\, c_{f2}\Gamma_{BF}dx\,. \qquad \text{(A-2)}$$

A.3 Bent Missile Terms

$$J_{1B} = \int_{x_0}^{x_2} c_{f1}\left(\Gamma_B + \Gamma_{BF}\right)\, dx \qquad J_{4B} = \int_{x_0}^{x_3} \left[c_{f2}\left(\Gamma_B + \Gamma_{BF}\right) - c_{f1}\delta_{EB}\right]\, xdx$$

$$J_{2B} = \int_{x_0}^{x_3} \left[c_{f2}\left(\Gamma_B + \Gamma_{BF}\right) - c_{f1}\delta_{EB}\right]\, dx \qquad J_{5B} = \int_{x_0}^{x_3} c_D\left(\delta_{EB} - \delta_{cB}\right)dx + \left[\delta_{EB}\left(x_1\right) - \delta_{cB}\right]\, c_{Dbp}$$

$$J_{3B} = \int_{x_0}^{x_3} c_{f1}\left(\Gamma_B + \Gamma_{BF}\right)\, xdx \qquad J_{6B} = \left(1/L\right)\int_{x_1}^{x_2} x\delta_B\rho_1 dx$$

$$\delta_{cB} = \left(1/L\right)\int_{x_1}^{x_2} \delta_B\rho_1 dx \qquad J_{8B1} = -a_d\int_{x_1}^{x_2} \Gamma_B\rho_2 dx$$

$$I_{xB1} = \left(1/L\right)\int_{x_0}^{x_3} \left[\rho_1\delta_{EB}\overline{\delta}_{EB} + \left(\rho_2 a_d L\right)\Gamma_B\overline{\Gamma}_B\right]\, dx \qquad I_{xB2} = -6a_d\int_{x_0}^{x_3} \left[\rho_2\Gamma_B\overline{\Gamma}_B\right]\, dx\,. \tag{A-3}$$

Appendix B. Functions

$$\delta_c = (1/L)\int_{x_1}^{x_2} \delta_E \rho_1 dx \qquad J_4(t) = \int_{x_0}^{x_3} \left(c_{f2}\Gamma - c_{f1}\delta_E\right)\, x dx$$

$$J_1(t) = \int_{x_0}^{x_3} c_{f1}\Gamma dx \qquad J_5(t) = \int_{x_0}^{x_3} c_D\left(\delta_E - \delta_c\right)\, dx + \left[\delta_E(x_1) - \delta_c\right]\, c_{Dbp}$$

$$J_2(t) = \int_{x_0}^{x_3} \left(c_{f2}\Gamma - c_{f1}\delta_E\right)\, dx \qquad J_6(t) = (1/L)\int_{x_1}^{x_2} x\delta_E \rho_1 dx$$

$$J_3(t) = \int_{x_0}^{x_3} c_{f1}\Gamma x dx \qquad J_8(t) = a_d \int_{x_1}^{x_2} \left(\dot{\Gamma} - 2i\dot{\phi}\Gamma\right)\rho_2 dx. \qquad \text{(B-1)}$$

INTENTIONALLY LEFT BLANK.

Appendix C. Generalized Forces and Hermitian Polynomials

$$dQ_{1x} = \frac{dF_x}{dx}dx = -g_1 c_D(x)\ dx$$

$$dQ_{1y} + i dQ_{1z} = \left[\frac{dF_y}{dx} + i\frac{dF_z}{dx} + (-\psi + i\theta)\frac{dF_x}{dx}\right]dx$$

$$dQ_{2x} = \frac{dM_x}{dx}dx$$

$$dQ_{2y} + i dQ_{2z} = \left[x\left(\frac{dF_y}{dx} + i\frac{dF_z}{dx}\right) - \delta_E\frac{dF_x}{dx} - \theta\frac{dM_x}{dx}\right]dx$$

$$Q_{1x} = F_x$$

$$Q_{1y} + iQ_{1z} = F_y + iF_z + (-\psi + i\theta)F_x$$

$$Q_{2x} = M_x$$

$$Q_{2y} + iQ_{2z} = -i\left(M_y + iM_z - iF_x\delta_c\right) - \theta M_x$$

$$N_1 = 1 - 3z^2 + 2z^3 \qquad N_1' = 6\left(z^2 - z\right)$$

$$N_2 = L_e z(1-z)^2 \qquad N_2' = L_e\left(1 - 4z + 3z^2\right)$$

$$N_3 = z^2(3 - 2z) \qquad N_3' = 6\left(z - z^2\right)$$

$$N_4 = L_e z^2(z-1) \qquad N_4' = L_e\left(3z^2 - 2z\right). \qquad \text{(C-1)}$$

INTENTIONALLY LEFT BLANK.

Appendix D. Connector Coefficients for Equations (39–41)

D.1 Rod Parameters

$$\hat{a}^1_{qj} = L_e \int_0^1 \rho_1(x)\, N_q(z)\, dz \qquad x = L_e(z_j + z)$$

$$\hat{a}^2_{qj} = L_e \int_0^1 x\rho_1(x)\, N_q(z)\, dz \qquad z_j = (x_1/L_e) + j - 1$$

$$\hat{b}^2_{qj} = \int_0^1 \rho_2(x)\, N'_q(z)\, dz \qquad q = 1,\ 2,\ 3,\ 4. \tag{D-1}$$

For central element $r = \dfrac{n_j + 1}{2}$

$$\hat{a}^1_{1c} = \hat{a}^1_{1r} + 5\hat{a}^1_{3r} + 24L_e^{-1}\hat{a}^1_{4r} \qquad \hat{a}^1_{2c} = \hat{a}^1_{2r} + L_e\hat{a}^1_{3r} + 5\hat{a}^1_{4r}$$

For adjacent element $r = \dfrac{n_j + 3}{2}$

$$\hat{a}^1_{1a} = 5\hat{a}^1_{1r} + 24L_e^{-1}\hat{a}^1_{2r} \qquad \hat{a}^1_{2a} = L_e\hat{a}^1_{1r} + 5\hat{a}^1_{2r}$$
$$\hat{a}^1_{3a} = \hat{a}^1_{3r} \qquad \hat{a}^1_{4a} = \hat{a}^1_{4r},$$

$\hat{a}^2_{qc}$, $\hat{a}^2_{qa}$, $\hat{b}^2_{qc}$, and $\hat{b}^2_{qa}$ are computed from $\hat{a}^2_{qj}$ and $\hat{b}^2_{qj}$ in same manner as previously shown.

$$a_{11} = a_{12} = 0$$

$$n_t = 4 \qquad L_e = L$$

$$a_{13} = \hat{a}^1_{1c} \qquad a_{14} = \hat{a}^1_{2c}$$

$$n_t = 8 \qquad L_e = L/3$$

$$a_{13} = \hat{a}^1_{11} \quad a_{14} = \hat{a}^1_{21} \qquad a_{15} = \hat{a}^1_{31} + \hat{a}^1_{1c} + \hat{a}^1_{1a} \qquad a_{16} = \hat{a}^1_{41} + \hat{a}^1_{2c} + \hat{a}^1_{2a} \qquad a_{17} = \hat{a}^1_{3a} \qquad a_{18} = \hat{a}^1_{4a}$$

$$n_t = 12 \qquad L_e = L/5$$

$$a_{13} = \hat{a}^1_{11} \qquad a_{14} = \hat{a}^1_{21} \qquad a_{15} = \hat{a}^1_{31} + \hat{a}^1_{12} \qquad a_{16} = \hat{a}^1_{41} + \hat{a}^1_{22}$$
$$a_{17} = \hat{a}^1_{32} + \hat{a}^1_{1c} + \hat{a}^1_{1a} \qquad a_{18} = \hat{a}^1_{42} + \hat{a}^1_{2c} + \hat{a}^1_{2a} \qquad a_{19} = \hat{a}^1_{3a} + \hat{a}^1_{15}$$
$$a_{1(10)} = \hat{a}^1_{4a} + \hat{a}^1_{25} \quad a_{1(11)} = \hat{a}^1_{35} \qquad a_{1(12)} = \hat{a}^1_{45}$$

$$n_t = 16 \qquad L_e = L/7$$

$$a_{13} = \hat{a}^1_{11} \qquad a_{14} = \hat{a}^1_{21} \qquad a_{15} = \hat{a}^1_{31} + \hat{a}^1_{12} \qquad a_{16} = \hat{a}^1_{41} + \hat{a}^1_{22} \qquad a_{17} = \hat{a}^1_{32} + \hat{a}^1_{13}$$

$$a_{18} = \hat{a}^1_{42} + \hat{a}^1_{23} \qquad a_{19} = \hat{a}^1_{33} + \hat{a}^1_{1c} + \hat{a}^1_{1a} \qquad a_{1(10)} = \hat{a}^1_{43} + \hat{a}^1_{2c} + \hat{a}^1_{2a} \qquad a_{1(11)} = \hat{a}^1_{3a} + \hat{a}^1_{16}$$

$$a_{1(12)} = \hat{a}^1_{4a} + \hat{a}^1_{26} \qquad a_{1(13)} = \hat{a}^1_{36} + \hat{a}^1_{17} \qquad a_{1(14)} = \hat{a}^1_{46} + \hat{a}^1_{27} \qquad a_{1(15)} = \hat{a}^1_{37} \qquad a_{1(16)} = \hat{a}^1_{47}$$

a_{2n} and b_{2n} are computed from $\hat{a}^2_{qj}$, $\hat{a}^2_{qc}$, $\hat{a}^2_{qa}$, $\hat{b}^2_{qj}$, $\hat{b}^2_{qc}$, and $\hat{b}^2_{qa}$ in the same manner as previously shown.

Appendix E. Connector Coefficients for Equations (42–44)

E.1 Rod Terms

$$\hat{f}_{qj}^{1} = \int_0^1 c_{f1}(x)\ N_q'(z)\ dz \qquad x = L_e(z_j + z)$$

$$\hat{g}_{qj}^{1} = \int_0^1 \left[c_{f2}(x)\ N_q'(z) - c_{f1}(x)\ N_q(z)\ L_e \right] dz \qquad z_j = (x_1/L_e) + j - 1$$

$$\hat{f}_{qj}^{2} = \int_0^1 \left[c_{f1}(x)\ N_q'(z) \right] x\,dz \qquad q = 1,\ 2,\ 3,\ 4$$

$$\hat{g}_{qj}^{2} = \int_0^1 \left[c_{f2}(x)\ N_q'(z) - c_{f1}(x)\ N_q(z)\ L_e \right] x\,dz, \tag{E-1}$$

f_{1n}, f_{2n}, g_{1n}, and g_{2n} are computed from $\hat{f}_{qj}^{1}$, $\hat{f}_{qj}^{2}$, $\hat{g}_{qj}^{1}$, and $\hat{g}_{qj}^{2}$ in the same manner as in appendix D.

E.2 Nonzero Aerodynamic Extension Terms

$$n_t = 4$$

$$f_{a13} = 24L_e^{-1}I_2 \qquad f_{a14} = I_1 + 5I_2$$

$$f_{a23} = 24L_e^{-1}I_{18} \qquad f_{a24} = I_{17} + 5I_{18}$$

$$g_{a13} = -I_1 - 5I_2 + 24L_e^{-1}(I_6 - I_4) \qquad g_{a14} = I_5 - I_3 - I_2L_e + 5(I_6 - I_4)$$

$$g_{a23} = -I_{17} - 5I_{18} + 24L_e^{-1}I_{16} \qquad g_{a24} = I_{15} - I_{18}L_e + 5I_{16}$$

$$h_{a3} = I_{ID} + 5I_{2D} + 24L_e^{-1}I_{4D} \qquad h_{a4} = I_{3DE} + L_eI_{2D} + 5I_{4D}$$

$$n_t \neq 4$$

$$f_{a14} = I_1 \qquad f_{a1n_t} = I_2$$

$$f_{a24} = I_{17} \qquad f_{a2n_t} = I_{18}$$

$$g_{a13} = -I_1 \qquad g_{a14} = I_5 - I_3 \qquad g_{a1(n_t-1)} = -I_2 \qquad g_{a1n_t} = I_6 - I_4$$

$$g_{a23} = -I_{17} \qquad g_{a24} = I_{15} \qquad g_{a1(n_t-1)} = -I_{18} \qquad g_{a1n_t} = I_{16}$$

$$h_{a3} = I_{ID} \qquad h_{a4} = I_{3D} \qquad h_{a(n_t-1)} = I_{2D} \qquad h_{an_t} = I_{4D}. \tag{E-2}$$

INTENTIONALLY LEFT BLANK.

Appendix F. Differential Equations Coefficients

F.1 Equation 44 m = 1, 2

$$R_{1n} = \left(md^2/L\right)\, a_{1n} \qquad R_{2n} = \left(md^2/L\right)\, \left[a_{2n} + \left(a_d L\right)\, b_{2n} + x_c a_{1n}\right]$$

$$S_{11} = \left(md\right)\, V + \left(g_1 d^2/V\right)\, c_2 \qquad S_{12} = x_c md^2$$

$$S_{1n} = -\left(g_1 d^2/V\right)\, \left(g_{1n} + g_{a1n}\right) \qquad S_{21} = \left(g_1 d^2/V\right)\, \left(c_4 - x_c c_2\right)$$

$$S_{22} = I_t + md^2 x_c^2 \qquad S_{2n} = -\left(g_1 d^2/V\right)\, \left(g_{2n} + g_{a2n}\right) - x_c S_{1n}$$

$$T_{11} = \left(g_1 d\right)\, \left(c_1 - C_D\right) \qquad T_{12} = \left(md\right)\, V$$

$$T_{1n} = -\left(g_1 d\right)\, \left(f_{1n} + f_{a1n}\right) \qquad T_{21} = \left(g_1 d\right)\, \left(c_3 - x_c c_1\right)$$

$$T_{2n} = -\left(g_1 d\right)\, \left(f_{2n} + f_{a2n} - C_D a_{1n} L^{-1} + h_{an}\right) - x_c T_{1n}$$

$$S^*_{2n} = -2\left(\, md^2\right)\, a_d b_{2n} \qquad T^*_{22} = -I_x$$

$$t_{D1} = \left(\dot{\phi}^2 - i\ddot{\phi}\right)\, \delta_{cB} \qquad t_{D2} = \left(\dot{\phi}^2 - i\ddot{\phi}\right)\, \left(J_{6B} - J_{8B1}\right)$$

$$t_{A1} = J_{1B} + i\, \left(\, \dot{\phi} d/V\right)\, J_{2B} \qquad t_{A2} = J_{3B} + i\left(\, \dot{\phi} d/V\right)\, J_{4B}$$

F.2 Equation 44 m = 3, 4…n_t

$$R_{mn} = \left(md^2/L\right)\, k_{mn}$$

$$S_{m1} = \left(md\right)\, V d_m - \left(g_1 d^2/V\right)\, \left(g_{m1} + g_{am1}\right) \qquad S_{m2} = R_{2m}$$

$$S_{mn} = -\left(g_1 d^2/V\right)\, \left(g_{mn} + g_{amn}\right) + \left(\, md^2/L\right)\, \left(2\omega_0^2/\omega_1\right)\, \hat{k} c_{mn}$$

$$T_{m1} = -\left(g_1 d\right)\, \left(f_{m1} + f_{am1} + C_D a_{1m} L^{-1}\right) \qquad T_{m2} = mdV a_{1m} L^{-1}$$

$$T_{mn} = -\left(g_1 d\right)\, \left(f_{mn} + f_{amn}\right) + \left(md^2/L\right)\, \omega_0^2 c_{mn} + 2\dot{\phi}^2 md^2 a_d b_{mn}$$

$$S^*_{mn} = -4\left(\, md^2\right)\, a_d b_{mn} \qquad T^*_{m2} = 2md^2 a_d b_{2m}$$

$$T^*_{mn} - -\left(md^2/L\right)\, \left(2\omega_0^2/\omega_1\right)\, \hat{k} c_{mn}$$

$$t_{mD} = \left(\dot{\phi}^2 - i\ddot{\phi}\right)\left(k_{Bm}/L + 2a_d b_{Bm}\right) - 4i\dot{\phi}^2 a_d b_{Bm}$$

$$t_{3A} = f_{B3} + I_{1B} + i\left(\, \dot{\phi} d/V\right)\, \left(g_{B3} + I_{5B}\right)$$

$$t_{4A} = f_{B4} + I_{3B} + i\left(\, \dot{\phi} d/V\right)\, \left(g_{B4} + I_{7B}\right)$$

$$t_{mA} = f_{Bm} + i\left(\dot{\phi}d/V\right)\, g_{Bm} \qquad 4 < m < n_t - 1$$

$$`\, t_{(n_t-1)A} = f_{B(n_t-1)} + I_2\Gamma_B(x_2) + i\left(\dot{\phi}d/V\right)\, \left(g_{B(n_t-1)} + I_6\Gamma_B(x_2)\right)$$

$$t_{n_tA} = f_{Bn_t} + I_4\Gamma_B(x_2) + i\left(\dot{\phi}d/V\right)\, \left(g_{Bn_t} + I_8\Gamma_B(x_2)\right)$$

For $n_j = 1 \quad n_t = 4 \quad m = 3,\ 4$

$$t_{mD} = \left(\dot{\phi}^2 - i\ddot{\phi}\right)\, k_{Bm}/L$$

$$t_{3A} = \hat{f}_{B1c} + I_{1B} + 5I_2\Gamma_B(x_2) + 24L_e^{-1}I_4\Gamma_B(x_2)$$
$$+ i\left(\dot{\phi}d/V\right)\, \left(\hat{g}_{B1c} + I_{5B} + 5I_6\Gamma_B(x_2) + 24L_e^{-1}I_8\Gamma_B(x_2)\right)$$

$$t_{4A} = \hat{f}_{B2c} + I_{3B} + L_eI_2\Gamma_B(x_2) + 5I_4\Gamma_B(x_2)$$
$$+ i\left(\dot{\phi}d/V\right)\, \left(\hat{g}_{B2c} + I_{7B} + L_eI_6\Gamma_B(x_2) + 5I_8\Gamma_B(x_2)\right). \qquad \text{(F-2)}$$

F.3 Quadratic Spin Equation (61)

$$J_7 = -(i/L)\int_{x_1}^{x_2}\left[\rho_1\dot{\delta}_E\bar{\delta}_E - \rho_2a_dL\left(\dot{\Gamma} + 4i\dot{\phi}\Gamma + iq_2\right)\,\bar{\Gamma}\right]\,dx$$

$$Q_D = -(i/L)\sum_{m=3}^{n_t}\sum_{n=3}^{n_t}\left[\left(a_{mn} - a_dLb_{mn}\right)\,\ddot{q}_m\bar{q}_n + 8i\dot{\phi}a_dLb_{mn}\dot{q}_m\bar{q}_n\right]$$

$$-(i/L)e^{-i\phi}\sum_{m=3}^{n_t}\left[\left(\bar{a}_{Bm} - a_dL\bar{b}_{Bm}\right)\,\left[\ddot{q}_m + \dot{\phi}^2q_m\right] + 8i\dot{\phi}a_dL\bar{b}_{Bm}\left(\dot{q}_n - i\dot{\phi}q_m\right)\right]$$

$$I_X = I_x + I_{xB} - \left(md^2/L\right)\,\mathrm{Re}\left\{4a_dL\sum_{m=3}^{n_t}\sum_{n=3}^{n_t}b_{mn}q_m\bar{q}_n + e^{-i\phi}\sum_{m=3}^{n_t}\left(\bar{a}_{Bm} - 3\left(a_dL\right)\bar{b}_{Bm}\right)\,q_m\right\}$$

$$I_{xB} = md^2\left(I_{xB1} + I_{xB2}\right). \qquad \text{(F-3)}$$

Appendix G. Flexing Motion Finite Element Method (FEM) Quantities

G.1 Kinetic and Potential Energy Coefficients

$$\hat{a}_{pqj} = L_e \int_0^1 \rho_1(x) N_p N_q dz$$

$$\hat{b}_{pqj} = L_e^{-1} \int_0^1 \rho_2(x) \frac{dN_p}{dz} \frac{dN_q}{dz} dz$$

$$\hat{c}_{pqj} = L_e^{-3} \int_0^1 \rho_3(x) \frac{d^2N_p}{dz^2} \frac{d^2N_q}{dz^2} dz. \qquad \text{(G-1)}$$

2×2 central element matrix $\quad r = \dfrac{n_j + 1}{2}$

$$\hat{a}_{11c} = \hat{a}_{11r} + 5(\hat{a}_{13r} + \hat{a}_{31r}) + 24L_e^{-1}(\hat{a}_{14r} + \hat{a}_{41r}) + 25\hat{a}_{33r} + 120L_e^{-1}(\hat{a}_{34r} + \hat{a}_{43r}) + (24)^2 \hat{a}_{44r} L_e^{-2}$$

$$\hat{a}_{12c} = \hat{a}_{12r} + L_e\hat{a}_{13r} + 5(\hat{a}_{14r} + \hat{a}_{32r}) + 24L_e^{-1}\hat{a}_{42r} + 5L_e\hat{a}_{33r} + 25\hat{a}_{34r} + 24\hat{a}_{43r} + 120L_e^{-1}\hat{a}_{44r}$$

$$\hat{a}_{21c} = \hat{a}_{21r} + 5(\hat{a}_{23r} + \hat{a}_{41r}) + 24L_e^{-1}\hat{a}_{24r} + L_e\hat{a}_{31r} + 5L_e\hat{a}_{33r} + 24\hat{a}_{34r} + 25\hat{a}_{43r} + 120L_e^{-1}\hat{a}_{44r}$$

$$\bar{a}_{22c} = \hat{a}_{22r} + L_e(\hat{a}_{23r} + \hat{a}_{32r}) + 5(\hat{a}_{24r} + \hat{a}_{42r}) + L_e^2\hat{a}_{33r} + 5L_e(\hat{a}_{34r} + \hat{a}_{43r}) + 25\hat{a}_{44r}$$

4×4 adjacent element matrix $\quad r = \dfrac{n_j + 3}{2}$

$$\hat{a}_{11a} = 25\hat{a}_{11r} + 120L_e^{-1}(\hat{a}_{12r} + \hat{a}_{21r}) + (24)^2 \hat{a}_{22r} L_e^{-2}$$

$$\hat{a}_{12a} = 5L_e\hat{a}_{11r} + 24\hat{a}_{21r} + 25\hat{a}_{12r} + 120L_e^{-1}\hat{a}_{22r}$$

$$\hat{a}_{21a} = 5L_e\hat{a}_{11r} + 25\hat{a}_{21r} + 24\hat{a}_{12r} + 120L_e^{-1}\hat{a}_{22r}$$

$$\hat{a}_{22a} = L_e^2\hat{a}_{11r} + 5L_e(\hat{a}_{12r} + \hat{a}_{21r}) + 25\hat{a}_{22r}$$

$$\hat{a}_{13a} = 5\hat{a}_{13r} + 24\hat{a}_{23r}L_e^{-1} \qquad \hat{a}_{31a} = 5\hat{a}_{31r} + 24\hat{a}_{32r}L_e^{-1}$$

$$\hat{a}_{14a} = 5\hat{a}_{14r} + 24\hat{a}_{24r}L_e^{-1} \qquad \hat{a}_{41a} = 5\hat{a}_{41r} + 24\hat{a}_{42r}L_e^{-1}$$

$$\hat{a}_{23a} = L_e\hat{a}_{13r} + 5\hat{a}_{23r} \qquad \hat{a}_{32a} = L_e\hat{a}_{31r} + 5\hat{a}_{32r}$$

$$\hat{a}_{24a} = L_e\hat{a}_{14r} + 5\hat{a}_{24r} \qquad \hat{a}_{42a} = L_e\hat{a}_{41r} + 5\hat{a}_{42r}$$

$$\hat{a}_{33a} = \hat{a}_{33r} \qquad \hat{a}_{34a} = \hat{a}_{34r}$$

$$\hat{a}_{43a} = \hat{a}_{43r} \qquad \hat{a}_{44a} = \hat{a}_{44r}$$

$\hat{b}_{pqc}$, $\hat{b}_{pqa}$, $\hat{c}_{pqc}$, and $\hat{c}_{pqa}$ are computed from $\hat{b}_{pqj}$ and $\hat{c}_{pqj}$ in the same manner as previously shown.

$$n_t = 4$$

$$L_e = L \qquad a_{mn} = \hat{a}_{(m-2)(n-2)c} \qquad m,n = 3,4$$

$$n_t = 8$$

$$L_e = L/3$$

$a_{33} = \hat{a}_{111}$ $a_{34} = \hat{a}_{121}$ $a_{35} = \hat{a}_{131}$ $a_{36} = \hat{a}_{141}$

$a_{43} = \hat{a}_{211}$ $a_{44} = \hat{a}_{221}$ $a_{45} = \hat{a}_{231}$ $a_{46} = \hat{a}_{241}$

$a_{53} = \hat{a}_{311}$ $a_{54} = \hat{a}_{321}$ $a_{55} = \hat{a}_{331} + \hat{a}_{11c} + \hat{a}_{11a}$ $a_{56} = \hat{a}_{341} + \hat{a}_{12c} + \hat{a}_{12a}$ $a_{57} = \hat{a}_{13a}$ $a_{58} = \hat{a}_{14a}$

$a_{63} = \hat{a}_{411}$ $a_{64} = \hat{a}_{421}$ $a_{65} = \hat{a}_{431} + \hat{a}_{21c} + \hat{a}_{21a}$ $a_{66} = \hat{a}_{441} + \hat{a}_{22c} + \hat{a}_{22a}$ $a_{67} = \hat{a}_{23a}$ $a_{68} = \hat{a}_{24a}$

$a_{75} = \hat{a}_{31a}$ $a_{76} = \hat{a}_{32a}$ $a_{77} = \hat{a}_{33a}$ $a_{78} = \hat{a}_{34a}$

$a_{85} = \hat{a}_{41a}$ $a_{86} = \hat{a}_{42a}$ $a_{87} = \hat{a}_{43a}$ $a_{88} = \hat{a}_{44a}$ other a_{mn}'s are zero

$$n_t = 12$$

$$L_e = L/5$$

$a_{33} = \hat{a}_{111}$ $a_{34} = \hat{a}_{121}$ $a_{35} = \hat{a}_{131}$ $a_{36} = \hat{a}_{141}$

$a_{43} = \hat{a}_{211}$ $a_{44} = \hat{a}_{221}$ $a_{45} = \hat{a}_{231}$ $a_{46} = \hat{a}_{241}$

$a_{53} = \hat{a}_{311}$ $a_{54} = \hat{a}_{321}$ $a_{55} = \hat{a}_{331} + \hat{a}_{112}$ $a_{56} = \hat{a}_{341} + \hat{a}_{122}$ $a_{57} = \hat{a}_{132}$ $a_{58} = \hat{a}_{142}$

$a_{63} = \hat{a}_{411}$ $a_{64} = \hat{a}_{421}$ $a_{65} = \hat{a}_{431} + \hat{a}_{212}$ $a_{66} = \hat{a}_{441} + \hat{a}_{222}$ $a_{67} = \hat{a}_{232}$ $a_{68} = \hat{a}_{242}$

$a_{75} = \hat{a}_{312}$ $a_{76} = \hat{a}_{322}$ $a_{77} = \hat{a}_{332} + \hat{a}_{11c} + \hat{a}_{11a}$ $a_{78} = \hat{a}_{342} + \hat{a}_{12c} + \hat{a}_{12a}$ $a_{79} = \hat{a}_{13a}$ $a_{7(10)} = \hat{a}_{14a}$

$a_{85} = \hat{a}_{412}$ $a_{86} = \hat{a}_{422}$ $a_{87} = \hat{a}_{432} + \hat{a}_{21c} + \hat{a}_{21a}$ $a_{88} = \hat{a}_{442} + \hat{a}_{22c} + \hat{a}_{22a}$ $a_{89} = \hat{a}_{23a}$ $a_{8(10)} = \hat{a}_{24a}$

$a_{97} = \hat{a}_{31a}$ $a_{98} = \hat{a}_{32a}$ $a_{99} = \hat{a}_{33a} + \hat{a}_{115}$ $a_{9(10)} = \hat{a}_{34a} + \hat{a}_{125}$ $a_{9(11)} = \hat{a}_{135}$ $a_{9(12)} = \hat{a}_{145}$

$a_{(10)7} = \hat{a}_{41a}$ $a_{(10)8} = \hat{a}_{42a}$ $a_{(10)9} = \hat{a}_{43a} + \hat{a}_{215}$ $a_{(10)10} = \hat{a}_{44a} + \hat{a}_{225}$ $a_{(10)11} = \hat{a}_{235}$ $a_{(10)12} = \hat{a}_{245}$

$a_{(11)9} = \hat{a}_{315}$ $a_{(11)10} = \hat{a}_{325}$ $a_{(11)11} = \hat{a}_{335}$ $a_{(11)12} = \hat{a}_{345}$

$a_{(12)9} = \hat{a}_{415}$ $a_{(12)10} = \hat{a}_{425}$ $a_{(12)11} = \hat{a}_{435}$ $a_{(12)12} = \hat{a}_{445}$ other a_{mn}'s are zero

$$n_t = 16$$

$$L_e = L/7$$

$a_{33} = \hat{a}_{111}$ $a_{34} = \hat{a}_{121}$ $a_{35} = \hat{a}_{131}$ $a_{36} = \hat{a}_{141}$

$a_{43} = \hat{a}_{211}$ $a_{44} = \hat{a}_{221}$ $a_{45} = \hat{a}_{231}$ $a_{46} = \hat{a}_{241}$

$a_{53} = \hat{a}_{311}$ $a_{54} = \hat{a}_{321}$ $a_{55} = \hat{a}_{331} + \hat{a}_{112}$ $a_{56} = \hat{a}_{341} + \hat{a}_{122}$ $a_{57} = \hat{a}_{132}$ $a_{58} = \hat{a}_{142}$

$a_{63} = \hat{a}_{411}$ $a_{64} = \hat{a}_{421}$ $a_{65} = \hat{a}_{431} + \hat{a}_{212}$ $a_{66} = \hat{a}_{441} + \hat{a}_{222}$ $a_{67} = \hat{a}_{232}$ $a_{68} = \hat{a}_{242}$

$a_{75} = \hat{a}_{312}$ $a_{76} = \hat{a}_{322}$ $a_{77} = \hat{a}_{332} + \hat{a}_{113}$ $a_{78} = \hat{a}_{342} + \hat{a}_{123}$ $a_{79} = \hat{a}_{133}$ $a_{7(10)} = \hat{a}_{143}$

$a_{85} = \hat{a}_{412}$ $a_{86} = \hat{a}_{422}$ $a_{87} = \hat{a}_{432} + \hat{a}_{213}$ $a_{88} = \hat{a}_{442} + \hat{a}_{223}$ $a_{89} = \hat{a}_{233}$ $a_{8(10)} = \hat{a}_{243}$

$a_{97} = \hat{a}_{313}$ $a_{98} = \hat{a}_{323}$ $a_{99} = \hat{a}_{333} + \hat{a}_{11c} + \hat{a}_{11a}$ $a_{9(10)} = \hat{a}_{343} + \hat{a}_{12c} + \hat{a}_{12a}$ $a_{9(11)} = \hat{a}_{13a}$ $a_{9(12)} = \hat{a}_{14a}$

$a_{(10)7} = \hat{a}_{413}$ $a_{(10)8} = \hat{a}_{423}$ $a_{(10)9} = \hat{a}_{433} + \hat{a}_{21c} + \hat{a}_{21a}$ $a_{(10)10} = \hat{a}_{443} + \hat{a}_{22c} + \hat{a}_{22a}$ $a_{(10)11} = \hat{a}_{23a}$ $a_{(10)12} = \hat{a}_{24a}$

$a_{(11)9} = \hat{a}_{31a}$ $a_{(11)10} = \hat{a}_{32a}$ $a_{(11)11} = \hat{a}_{33a} + \hat{a}_{116}$ $a_{(11)12} = \hat{a}_{34a} + \hat{a}_{126}$ $a_{(11)13} = \hat{a}_{136}$ $a_{(11)14} = \hat{a}_{146}$

$a_{(12)9} = \hat{a}_{41a}$ $a_{(12)10} = \hat{a}_{42a}$ $a_{(12)11} = \hat{a}_{43a} + \hat{a}_{216}$ $a_{(12)12} = \hat{a}_{44a} + \hat{a}_{226}$ $a_{(12)13} = \hat{a}_{236}$ $a_{(12)14} = \hat{a}_{246}$

$a_{(13)11} = \hat{a}_{316}$ $a_{(13)12} = \hat{a}_{326}$ $a_{(13)13} = \hat{a}_{336} + \hat{a}_{117}$ $a_{(13)14} = \hat{a}_{346} + \hat{a}_{127}$ $a_{(13)15} = \hat{a}_{137}$ $a_{(13)16} = \hat{a}_{147}$

$a_{(14)11} = \hat{a}_{416}$ $a_{(14)12} = \hat{a}_{426}$ $a_{(14)13} = \hat{a}_{436} + \hat{a}_{217}$ $a_{(14)14} = \hat{a}_{446} + \hat{f}_{227}$ $a_{(14)15} = \hat{a}_{237}$ $a_{(14)16} = \hat{a}_{247}$

$a_{(15)13} = \hat{a}_{317}$ $a_{(15)14} = \hat{a}_{327}$ $a_{(15)15} = \hat{a}_{337}$ $a_{(15)16} = \hat{a}_{347}$

$a_{(16)13} = \hat{a}_{417}$ $a_{(16)14} = \hat{a}_{427}$ $a_{(16)15} = \hat{a}_{437}$ $a_{(16)16} = \hat{a}_{447}$ other a_{mn} 's are zero

b_{mn} and c_{mn} computed from $\hat{b}_{pqj}$, $\hat{b}_{pqc}$, $\hat{b}_{pqa}$, $\hat{c}_{pqj}$, $\hat{c}_{pqc}$, and $\hat{c}_{pqa}$ in the same manner as previously shown.

$$k_{mn} = a_{mn} + (a_d L)\, b_{mn}$$

G.2 Kinetic Energy FEM Vectors

$$\hat{a}_{Bpj} = L_e \int_0^1 \rho_1(x)\, \delta_{EB}(x)\, N_p(z)\, dz \qquad x = L_e(z_j + z)$$

$$\hat{b}_{Bpj} = \int_0^1 \rho_2(x)\, \Gamma_B(x)\, N_p'(z)\, dz \qquad z_j = (x_1/L_e) + j - 1. \qquad \text{(G-2)}$$

a_{Bm} and $b_{\cdot Bm}$ are computed from $\hat{a}_{Bpj}$ and $\hat{b}_{Bpj}$ in the same manner as a_{1n} was computed from $\hat{a}^1_{nj}$,

$$k_{Bm} = a_{Bm} + (a_d L)\, b_{Bm}\,.$$

G.3 Rod Aerodynamic Force Terms

$$\hat{f}_{pqj} = \int_0^1 c_{f1}(x)\ N_q' N_p(z)\ dz \qquad x = L_e(z_j + z)$$

$$\hat{g}_{pqj} = \int_0^1 \left[c_{f2}(x)\ N_q'(z) - c_{f1}(x)\ N_q(z)\ L_e \right] N_p(z)\ dz \qquad z_j = (x_1/L_e) + j - 1$$

$$p, q = 1,\ 2,\ 3,\ 4. \qquad \text{(G-3)}$$

f_{mn} and g_{mn} are computed from $\hat{f}_{pqj}$ and $\hat{g}_{pqj}$ in the same manner as a_{mn} was computed from $\hat{a}_{pqj}$.

$$\hat{f}_{pj1} = -L_e \int_0^1 c_{f1}(x)\ N_p(z)\ dz \qquad x = L_e(z_j + z)$$

$$\hat{g}_{pj1} = -L_e \int_0^1 c_{f3}(x)\ N_p(z)\ dz \qquad z_j = (x_1/L_e) + j - 1$$

$$c_{f3}(x) = 2c_{f2} - x c_{f1} \qquad p = 1,\ 2,\ 3,\ 4$$

$$\hat{f}_{Bpj} = L_e \int_0^1 c_{f1}(x)\ \left[\Gamma_B(x) + \Gamma_{BF}(x) \right] N_p(z)\ dz$$

$$\hat{g}_{Bpj} = L_e \int_0^1 c_{f2}(x)\ \left[\Gamma_B(x) + \Gamma_{BF}(x) \right]\ (x)\ N_p(z)\ dz$$

f_{m1}, g_{m1}, f_{Bm}, and g_{Bm} are computed from $\hat{f}_{pj1}$, $\hat{g}_{pj1}$, $\hat{f}_{Bpj}$, and $\hat{g}_{Bpj}$ in the same manner as a_{1n} was computed from $\hat{a}^1_{nj}$. All other f_{m1}, g_{m1}, f_{Bm}, and g_{Bm}'s are zero.

G.4 Nonzero Aerodynamic Extension Terms

$$n_t = 4$$

$$f_{a31} = -\left[I_1 + 5I_2 + 24L_e^{-1} I_4 \right] \qquad f_{a33} = 24L_e^{-1} \left[5(I_2 + I_{2D}) + 24L_e^{-1} I_4 \right]$$

$$f_{a34} = \left[I_1 + 25I_2 + 24I_{2D} + 120L_e^{-1}(I_4 + I_{4D}) \right] \qquad f_{a41} = -\left[I_3 + L_e I_2 + 5I_4 \right]$$

$$f_{a43} = \left[c_{Dbp} + 24I_2 + 25I_{2D} + 120L_e^{-1}(I_4 + I_{4D}) \right] \qquad f_{a44} = \left[I_3 + 5L_e(I_2 + I_{2D}) + 25(I_4 + I_{4D}) \right]$$

$$f_{aB3} = I_1 \Gamma_B(x_1) + 5I_2 \Gamma_B(x_2) + 24L_e^{-1} I_4 \Gamma_B(x_2) + I_{1BF} \qquad f_{aB4} = I_5 \Gamma_B(x_1) + 5I_6 \Gamma_B(x_2) + 24L_e^{-1} I_8 \Gamma_B + I_{3BF}$$

$$n_t \neq 4$$

$$f_{a31} = -I_1 \qquad f_{a34} = I_1 \qquad f_{a43} = c_{Dbp} \qquad f_{a41} = -I_3 \qquad f_{a44} = I_3$$

$$f_{a(n_t-1)1} = -I_2 \qquad f_{a(n_t-1)n_t} = I_2 \qquad f_{an_t(n_t-1)} = I_{2D} \qquad f_{a(n_t)1} = -I_4 \qquad f_{an_tn_t} = I_4 + I_{4D}$$

$$f_{aB3} = I_1\Gamma_B(x_1) + I_{1BF} \quad f_{aB4} = I_3\Gamma_B(x_1) + I_{3BF} \quad f_{aB(n_t-1)} = I_2\Gamma_B(x_2) \quad f_{aBn_t} = I_4\Gamma_B(x_2)$$

other f_{Amn} 's are zero

$$n_t = 4$$

$$g_{a31} = -\left[I_{11} + 5I_{12} + 24L_e^{-2}I_{14}\right] \qquad g_{a33} = -\left[I_1 + 25I_2 + 120L_e^{-1}(2I_4 - I_6) + (24)^2 L_e^{-2}(I_{10} - I_8)\right]$$

$$g_{a34} = -\left[I_3 - I_5 + 5L_eI_2 + 24(2I_4 - I_6) + 25(I_{10} - I_8)\right]$$

$$g_{a41} = -\left[I_{13} + L_eI_{12} + 5I_{14}\right] \qquad g_{a43} = -\left[I_3 + 5L_eI_2 + 24(2I_4 - I_6) + 120L_e^{-1}(I_{10} - I_8)\right]$$

$$g_{a44} = -\left[I_9 - I_7 + L_e^2I_2 + 5L_e(2I_4 - I_6) + 25(I_{10} - I_8)\right]$$

$$g_{aB3} = I_5\Gamma_B(x_1) + 5I_6\Gamma_B(x_2) + 24L_e^{-1}I_8\Gamma_B(x_2) + I_{5BF}$$

$$g_{aB4} = I_7\Gamma_B(x_1) + L_eI_6\Gamma_B(x_2) + 5I_8\Gamma_B(x_2) + I_{7BF}$$

$$n_t \neq 4$$

$$g_{a31} = -I_{11} \qquad g_{a33} = -I_1 \qquad g_{a34} = I_5 - I_3$$

$$g_{a41} = -I_{13} \qquad g_{a43} = -I_3 \qquad g_{a44} = I_7 - I_9$$

$$g_{a(n_n-1)1} = -I_{12} \qquad {}_{a(n_n-1)(n_n-1)} = -I_2 \qquad g_{a(n_n-1)(n_n)} = I_6 - I_4$$

$$g_{a(n_t)1} = -I_{14} \qquad g_{a(n_t)(n_t-1)} = -I_4 \qquad g_{a(n_t)(n_t)} = I_8 - I_{10}$$

$$g_{aB3} = I_5\Gamma_B(x_1) + I_{5BF} \quad g_{aB4} = I_7\Gamma_B(x_1) + I_{7BF} \quad g_{aB(n_t-1)} = I_6\Gamma_B(x_2) \quad g_{aBn_t} = I_8\Gamma_B(x_2)$$

other g_{amn} 's are zero . (G-4)

INTENTIONALLY LEFT BLANK.

Appendix H. Finned Missile Parameters

$\rho_1 = \rho_2 = \rho_3 = 1$ $\quad x_c = 0$

$L = 20$ $\quad V = 6000$ ft/s

$d = 0.35$ ft. $\quad \rho = 0.002$ slugs/ft^3

$m = 3.50$ slug $\quad x_{01} = x_{23} = 1$

$I_x = 0.054$ slug-ft^2 $\quad a_s = 1100$ ft/s

$I_t = 14.318$ slug-ft^2 $\quad a_L = 2\left[\sqrt{(V/a_s)^2 - 1}\right]^{-1}$

$$c_{f1} = 4(11 - x) \qquad 10 < x \le 11$$
$$= e^{2(x-10)} \qquad -5 < x \le 10$$
$$= -(2/\pi)(15 + 3x)\, a_L \qquad -7 < x \le -5$$
$$= (12/\pi)\, a_L \qquad -11 \le x \le -7$$

$$c_{f2} = 2(11 - x)^2 \qquad 10 < x \le 11$$
$$= 2 + 0.5\left(1 - e^{2(x-10)}\right) \qquad -5 < x \le 10$$
$$= 2.5 + (1/3\pi)\ (15 + 3x)^2\, a_L \qquad -7 < x \le -5$$
$$= 2.5 - (12/\pi)\ (6 + x)\ a_L \qquad -11 \le x \le -7$$

$$c_D = (0.30)\ (11 - x) \qquad 10 < x \le 11$$
$$= 0 \qquad x \le 10$$

$C_{Dbp} = 0.14$ $\quad C_{\ell p} = -18$

$d_{12} = 10^{-3}$ $\quad d_{22} = -0.25 \times 10^{-5}$

$C_{N\alpha} = 9.7$ $\quad C_{M\alpha} = -34.4$

$C_{Mq} = -980$ $\quad C_{M\dot{\alpha}} = -190$

INTENTIONALLY LEFT BLANK.

List of Symbols, Abbreviations, and Acronyms

$c_{fj}(x)$	aerodynamic force distributions functions
d	rod diameter
E	Young's modulus
F	$F_y + iF_z$ complex transverse aerodynamic force
a_d	$(16L)^{-1}$
g_l	$g_l \quad \rho V^2 S/2$
I	$(d)^4 \iint y^2 dydz = (d)^4 \iint z^2 dydz$, area moment of rod
I_x	axial moment of inertia of projectile
I_t	transverse moment of inertia of projectile
$\hat{k}$	beam damping coefficient
L	rod length / rod diameter
m	projectile mass
n_j	number of rod elements
n_t	$2n_j + 2$
p	projectile spin
q_l	$\beta + i\alpha$, complex angle of attack of central disk (nsc)
q_{le}	$\psi - i\theta$ complex yaw and pitch of central disk (nsc)
q_2	$\dot{\psi} - i\dot{\theta}$ complex yaw and pitch rate of central disk (nsc)
q_n	$n = 3.4 \ldots n_t$ FEM connectors (nsc)
q_{bn}	$n = 3.4 \ldots n_t$ FEM connectors (bfc)
L_e	L/n_j
S	$\pi d^2/4$

T total kinetic energy

T_d kinetic energy of disk at x with thickness dx

V magnitude of projectile velocity

x_1, x_2 location of beam ends

x_{01}, x_{23} dimensionless length of fore and aft aerodynamic extensions

x_c axial location of center of mass

α angle of attack of central disk

β angle of sideslip of central disk

Γ $\dfrac{\partial \delta_E}{\partial x}$, complex cant of disk

ε_M maximum strain of rod

δ_c $L^{-1}\int_{x_1}^{x_2} \delta_E dx$, lateral location of missile's cm

δ_E $\delta_{Ey} + i\delta_{Ez}$, lateral displacement of disk (nsc)

ϕ roll angle

$\dot{\phi}_k$ frequency of k-th mode

λ_k damping of k-th mode

ρ air density

ρ_j axial variation of mass, moment of inertia, elasticity

σ ω_1/ω_R

$\omega_0^2 =$ $E_0 I_0 (L/md)$

ω_1 lowest elastic frequency of beam in vacuum

ω_R rigid projectile zero-spin frequency

$\vec{F} =$ (F_x, F_y, F_z), aerodynamic force exerted on missile (nsc)

$\vec{M} =$ (M_x, M_y, M_z), aerodynamic moment exerted on missile (nsc)

$\mathrm{Re}\{z\}$ real part of z

$\mathrm{Im}\{z\}$ imaginary part of z

Carat superscript denotes quantity for a single element

Tilde superscript denotes elastic parameter for bent missile

B subscript denotes parameter for bent projectile

BF subscript denotes bent fin parameter

E subscript denotes an elastic coordinate parameter (nsc)

T subscript denotes trim motion parameter

b subscript denotes an elastic coordinate parameter (bfc)

(bfc) body-fixed coordinates

(efc) earth-fixed coordinates

(nsf) non-spinning coordinates

NO. OF COPIES	ORGANIZATION
1 (PDF ONLY)	DEFENSE TECHNICAL INFORMATION CTR DTIC OCA 8725 JOHN J KINGMAN RD STE 0944 FT BELVOIR VA 22060-6218
1	COMMANDING GENERAL US ARMY MATERIEL CMD AMCRDA TF 5001 EISENHOWER AVE ALEXANDRIA VA 22333-0001
1	INST FOR ADVNCD TCHNLGY THE UNIV OF TEXAS AT AUSTIN 3925 W BRAKER LN STE 400 AUSTIN TX 78759-5316
1	US MILITARY ACADEMY MATH SCI CTR EXCELLENCE MADN MATH THAYER HALL WEST POINT NY 10996-1786
1	DIRECTOR US ARMY RESEARCH LAB AMSRD ARL CS IS R 2800 POWDER MILL RD ADELPHI MD 20783-1197
3	DIRECTOR US ARMY RESEARCH LAB AMSRD ARL CI OK TL 2800 POWDER MILL RD ADELPHI MD 20783-1197
3	DIRECTOR US ARMY RESEARCH LAB AMSRD ARL CS IS T 2800 POWDER MILL RD ADELPHI MD 20783-1197

NO. OF COPIES	ORGANIZATION
	ABERDEEN PROVING GROUND
1	DIR USARL AMSRD ARL CI OK TP (BLDG 4600)

NO. OF COPIES	ORGANIZATION
1	COMMANDER US ARMY ARDEC TECHNICAL LIBRARY PICATINNY ARSENAL NJ 07806-5000
1	COMMANDER US NAVAL SURFACE WEAPONS WARFARE CENTER T PEPITONE MS MC K21 DAHLGREN VA 22448
1	TECHNICAL DIRECTOR US ARMY ARDEC AMSTA AR TD PICATINNY ARSENAL NJ 07806-5000
1	HQ USAMC PRNCPL DPTY FOR TECHLGY ALEXANDRIA VA 22333-0001
12	COMMANDER US ARMY ARDEC AET A C NG J GRAU S KAHN H HUDGINS M AMORUSO E BROWN B WONG W TOLEDO S CHUNG C LIVECCHIA G MALEJKO J WHYTE PICATINNY ARSENAL NJ 07806-5000
3	COMMANDER US ARMY ARDEC SMCAR CCH V B KONRAD E FENNELL T LOUZERIO PICATINNY ARSENAL NJ 07806-5000
4	COMMANDER US ARMY ARDEC SMCAR FSE A GRAF D LADD E ANDRICOPOULIS K CHEUNG PICATINNY ARSENAL NJ 07806-5000
6	COMMANDER US ARMY ARDEC SMCAR CCL D F PUZYCKI D CONWAY D DAVIS K HAYES M PINCAY W SCHUFF PICATINNY ARSENAL NJ 07806-5000
3	DIRECTOR US ARMY RESEARCH OFC G ANDERSON K CLARK T DOLIGOWSKI PO BOX 12211 RESEARCH TRIANGLE PARK NC 27709-2211
2	COMMANDER US NAVAL SURFC WEAPONS CTR CODE DK20 MOORE CODE DK20 DEVAN DAHLGREN VA 22448-5000
2	COMMANDER WHITE OAK LABORATORY US NSWC APPLIED MATH BR CODE R44 PRIOLO CODE R44 WARDLAW SILVER SPRING MD 20903-5000
1	COMMANDER US ARMY AVN AND MIS CMND AMSAM RD SS AT W WALKER REDSTONE ARSENAL AL 35898-5010

NO. OF
COPIES ORGANIZATION

4 COMMANDER
US AIR FORCE ARMAMENT LAB
AFATL FXA
B SIMPSON
G ASATE
R ABELGREN
G WINCHENBACK
EGLIN AFB FL 32542-5434

2 DIRECTOR
SANDIA NATIONAL LAB
W OBERKAMPF
W WOLFE
DIVISION 5800
ALBUQUERQUE NM 87185

1 DIRECTOR
LOS ALAMOS NATIONAL LAB
MS G770 W HOGAN
LOS ALAMOS NM 87545

1 DIRECTOR
NASA AMES RESEARCH CTR
MS 258 1 L SCHIFF
MOFFETT FIELD CA 94035

1 DIRECTOR
NASA LANGLEY RESEARCH CTR
M HEMSCH
LANGLEY STATION
HAMPTON VA 23665

1 MASSACHUSETTS INST OF TECH
DEPT OF AERONAUTICS AND
ASTRONAUTICS
E COVERT
77 MASSACHUSETTS AVE
CAMBRIDGE MA 02139

1 ARROW TECHLGY ASSOC INC
R WHYTE
PO BOX 4218
BURLINGTON VT 05401-4218

2 C H MURPHY
PO BOX 269
UPPER FALLS MD 21156

2 W H MERMAGEN
4149 U WAY
HAVRE DE GRACE MD 21078

NO. OF
COPIES ORGANIZATION

1 DR W STUREK
3500 CARSINWOOD DR
ABERDEEN MD 21001-1412

1 OREGON STATE UNIV
DEPT OF MECH ENGR
DR M COSTELLO
CORVALLIS OR 97331

ABERDEEN PROVING GROUND

4 COMMANDER
US ARMY ARDEC
SMCAR DSD T
R LIESKE
F MIRABELLE
J WHITESIDE
J MATTS
APG MD 21005

26 DIR USARL
AMSRD ARL CI H
C NIETUBICZ
AMSRD ARL HR SC
D SAVICK
AMSRD ARL SL BE
A MIKHAIL
AMSRD ARL WM
E SCHMIDT
AMSRD ARL WM B
A HORST
AMSRD ARL WM BA
W D AMICO
B DAVIS
T HAWKINS
AMSRD ARL WM BC
M BUNDY
G COOPER
W DRYSDALE
J GARNER
B GUIDOS
B OSKAY
P PLOSTINS
J SAHU
K SOENCKSEN
P WEINACHT
S WILKERSON
AMSRD ARL WM BD
T MINOR

NO. OF
COPIES ORGANIZATION

AMSRD ARL WM BF
H EDGE
AMSRD ARL WM T
B BURNS
AMSRD ARL WM TC
R COATES
W DE ROSSET
R MUDD
AMSRD ARL WM TD
E RAPACKI

NO. OF COPIES	ORGANIZATION
1	DEFENSE RESEARCH ESTABLISHMENT VALCARTIER DELIVERY SYSTEM DIVISION A D DUPUIS 2459 PIE XI NORD VAL BELAIR QUEBEC CANADA